energies

MDPI

Article

Incorporating Location Aspects in Process Integration Methodology

Hür Bütün *, Ivan Kantor and François Maréchal

Industrial Process and Energy Systems Engineering (IPESE), École Polytechnique Fédérale de Lausanne, 1951 Sion, Switzerland

* Correspondence: hur.butun@epfl.ch

Received: 28 June 2019; Accepted: 21 August 2019; Published: 29 August 2019

Abstract: The large potential for waste resource and heat recovery in industry has been motivating research toward increasing efficiency. Process integration methods have proven to be effective tools in improving industrial sites while decreasing their resource and energy consumption; however, location aspects and their impact are generally overlooked. This paper presents a method based on process integration, which considers the location of plants. The impact of the locations is included within the mixed integer linear programming framework in the form of heat losses, temperature and pressure drop, and piping cost. The objective function is selected as minimisation of the total cost of the system excluding piping cost and ϵ-constraints are applied on the piping cost to systematically generate multiple solutions. The method is applied to a case study with industrial plants from different sectors. First, the interaction between two plants and their utility integration are illustrated, depending on the piping cost limit which results in the heat pump and boiler on one site being gradually replaced by excess heat recovered from the other plant. Then, the optimisation of the whole system is carried out, as a large-scale application. At low piping cost allowances, heat is shared through high pressure steam in above-ground pipes, while at higher piping cost limits the system switches toward lower pressure steam sharing in underground pipes. Compared to the business-as-usual operation of the sites, the optimal solution obtained with the proposed method leads to 20% reduction in the overall cost of the system, including the piping cost. Further reduction in the cost is possible using a state of the art method but the technical and economic feasibility is not guaranteed. Thus, the present work provides a tool to find optimal industrial symbiosis solutions under different investment limits on the infrastructure between plants.

Keywords: industrial excess heat; process integration; location aspects; piping; heat losses; mixed integer linear programming

1. Introduction

Initially motivated by fluctuating energy prices, and more recently by environmental concerns, energy efficiency remains a focus of regulations, such as the Europe 2020 goals [1]. Industrial energy consumption accounts for 40% of the world [2] and 26% of the European energy consumption [3], making it one of the key sectors for increasing energy efficiency. Energy consumption in industry is mostly in the form of heat; thus, energy efficiency improvements imposed by these regulations can only be achieved by using heat more efficiently within the system.

Waste heat in industry is often defined as heat discharged to environment from the cooling systems (e.g., cooling towers) as well as the energy conversion technologies (e.g., boilers) in the form of heat losses. However, according to Bendig et al. [4], this is classified as excess heat and waste heat is only the part which cannot be recovered within the process, by another process or by using an energy conversion system. This convention is used throughout this work.

According to Reference [5], industrial excess heat accounts for 5–30% of the industrial energy consumption in different countries, averaging 22% in the EU which corresponds to 5–6% of the overall consumption. There are several options for valorisation of excess heat including direct heat recovery within a process, integration of energy conversion technologies (e.g., organic Rankine cycles) and heat recovery through other processes. Bendig et al. [4] suggested that a hierarchy is required between those options. Direct heat recovery is the most preferable since it typically requires the least investment and yields the largest improvement. Following this, remaining heat can be upgraded by heat pumps (HPs), transferred to another process or converted to another form, for example by using an organic Rankine cycle.

The International Energy Agency (IEA) classifies excess heat potential into theoretical, technical and economic potential [6]. Theoretical potential corresponds to the thermodynamic potential without considering the technologies for heat recovery. Technical potential takes into account the availability of technologies for heat recovery. For example, although the steel industry has large heat losses at high temperatures, the technical potential is low since technologies to recover heat from solids are not well developed. Finally, economic potential, leading to the heat recovery options the industries would be willing to invest in, accounts for the cost of heat recovery. Thus, when energy efficiency improvement options are considered, it is crucial to assess the technical and economic feasibility.

This paper, motivated by the high excess heat potential in industry and the importance of identifying economically feasible solutions, presents a novel methodology to determine heat and resource recovery within and between industrial processes. Instead of imposing a predefined hierarchy between the heat recovery options, the method introduces location aspects in process integration (PI) to obtain the optimal path for heat recovery under different investment cost limits on piping. Section 2 covers the methods available in the literature for improving industrial energy efficiency, Section 3 explains the method by going through the formulation in detail, Section 4 presents the case study that is used as a proof of concept, Section 5 discusses the results and Section 6 draws the conclusions of this work.

2. State of the Art

PI is a domain in energy efficiency research which aims to increase the heat and material recovery between processes and therefore reduce external resource dependency and energy supplied by fossil fuel-based technologies such as natural gas boilers. PI has been a research-intensive field since the oil crisis in the early 1970s. Although industrial energy efficiency was the main motivation for PI, it has also been used in urban energy system design [7], biomass conversion systems [8] and large-scale energy planning. The methods used in PI are classified in two main groups—namely graphical and mathematical programming (MP) methods.

Graphical methods in PI are based on pinch analysis (PA), which divide the system into hot (i.e., heat source) and cold streams (i.e., heat sink), aiming to maximise the heat exchange between them to minimise the hot and cold utility requirements. PA was first developed by Linnhoff and Hindmarsh [9] for a single industrial process. Afterwards, it was extended to total site analysis (TSA) in which the system consists of several production processes [10]. In PA, direct heat exchange between processes is considered. However, such exchanges may be problematic because of startup and shutdown dynamics or plant layout. Using utility systems for exchanges between the processes can solve those problems, since they have more operational flexibility. Hui and Ahmad [11] proposed a TSA method using utility systems. They considered the use of steam as an intermediate fluid for the exchange between processes. The capital cost of the heat exchanger network (HEN) was also included in their analysis while being ignored in the previous TSA methods. The design of utility systems is crucial in TSA as they commonly include centralised supply of heat and power to several plants. Pirmohamadi et al. [12] studied the optimal design of cogeneration systems in total sites. The method was based on site utility grand composite curves and aimed at maximising the exergy efficiency of the overall system. Short-term and seasonal storage play an important role in inter-plant heat recovery

in the case of multi-period problems. Liew et al. [13] extended the TSA methodology into seasonal total site heat storage cascade to model energy flows between sites and storage systems to determine the required storage size. Exchange between multiple plants brings about other challenges, such as process control and safety. Song et al., proposed a strategy to divide large-scale TSA problems into smaller sections to cope with these issues [14]. TSA was applied in each section to obtain the total inter-plant heat recovery. In inter-plant heat exchange, connections between plants can be in different configurations such as series, parallel or split. In their TSA-based method, Wang et al. [15] identified the excess heat of the plants and analysed inter-plant recovery using different connection patterns. The parallel pattern yielded higher heat recovery, while coming at a higher investment cost.

When the excess heat from plants is identified manually, it is critical to decide which streams participate in inter-plant transfer. A strategy to select such streams was presented by Song et al. [16]. They also introduced the concept of inter-plant shifted composite curves to maximise heat recovery using minimum heat capacity flowrate intermediate circuits. Hackl et al. [17] studied heat recovery in industrial clusters using TSA and intermediate fluids. The energy consumption of the cluster was reduced by introducing a hot water loop between plants. While TSA helps to identify the targets of energy requirements of multiple processes/plants, it brings about challenges in implementation due to the variety of plants/companies involved in the exchange. A method to overcome such challenges was developed by Hackl and Harvey [18]. In the first step of their method, TSA was used to find the total site targets, while in the second step the number of plants/companies involved in inter-plant heat integration was minimised and the investment required for the integration was split into periods. Industrial excess heat can also be valorised in a district heating network (DHN) as well as other plants. Morandin et al. [19] considered a case with an industrial cluster and a DHN. They concluded that cluster-wide heat collection yields better integration with the DHNs than connecting each site individually. Although using TSA energy targets for several plants have been identified, most methods ignore the distance between them. Chew et al. [20] listed layout as one of the main issues in implementing total site heat integration. They also recommended including piping cost for better analysis of inter-plant heat integration [17] and performing heat recovery through DHNs [19]. Liew et al. [21] added layout aspects in TSA by considering heat losses, temperature and pressure drop. First, the heat cascade was constructed using the problem table method of [9]. Afterwards, the corresponding heat losses, pressure and temperature drop were calculated and the streams in the problem table method were corrected accordingly. Finally, the heat cascade re-formulated with the new temperatures and heat loads.

Even though PA-based methods are effective in obtaining targets for total sites, when the number of plants and utility systems increase, they generally fail to obtain optimal solutions [15]. MP-based methods emerged to fill this gap and now dominate the field. Most of the early work focused on utility integration [22] and heat load distribution [23]. As heat integration measures require modifications in the heat exchangers, HEN synthesis was also included in some of the methods [24]. Despite the fact that inter-plant heat transfer directly with process streams is considered impractical in most studies, some methods available in the literature still considered it as an option. Zhang et al. [25] introduced a HEN optimisation method for hot direct discharges/feeds between plants. A larger heat recovery was achieved by using process streams directly instead of intermediate fluids; however, issues regarding the implementation of such exchanges were not addressed. Direct heat exchange between processes requires more piping than using an intermediate fluid and hence a higher piping investment cost. Wang et al., studied the heat integration of direct, indirect and combined methods of multiple plants [26]. They concluded that direct exchange is most beneficial method for short distances while combined methods are best for medium distances and indirect transfer should be used for long distances. However, the conclusion was case-dependent and could not be generalised.

The main focus in inter-plant heat integration is excess heat recovery between plants. Since different processes have different pinch temperatures, the excess heat of one plant can be useful for another one. Based on this phenomenon, Rodera and Bagajewicz developed a method for optimal

integration of intermediate fluids in inter-plant heat transfer [27]. First, the targets for inter-plant exchange were identified using linear programming (LP) and source and sink plants were determined. Then, the optimal placement of the intermediate fluid circuit was identified using a mixed integer linear programming (MILP) formulation. Afterwards, the method was extended from two plants to n-plants [28]. When plants with similar pinch points are considered, recovering heat between them using an intermediate fluid might not be feasible. Building on previous work of Reference [28], Bagajewicz and Barbaro developed a method which uses HPs to upgrade the temperature of the excess heat from one plant and use it elsewhere [29].

Stijepovic and Linke also worked on optimal heat recovery in industrial zones focusing on excess heat [30]. They identified the excess heat potential of the plants manually and calculated the maximum heat recovery potential using LP. Finally the optimal heat recovery network was found using a mixed integer non-linear programming formulation. However, intra-plant process integration and improvements through more efficient energy conversion technologies were not included in the method. The layout constraints or location aspects were considered directly or indirectly in several methods. Kantor et al. [31] formulated the problem as a set of nodes and connections between them. The location aspects were included by adding the cost of resource transportation. Transportation methods were defined for each material sharing potential and an appropriate method for each was established as a result of the optimisation. Becker and Maréchal [32] proposed a MILP method to divide the system into smaller subsystems based on their locations. The subsystems were allowed to exchange heat only using heat transfer systems represented by intermediate fluids. This way, direct heat exchange over long distances was prevented. Pouransari and Maréchal [33] extended the previous problem to a heat load distribution (HLD) formulation. Implementation of sub-systems helped solving large-scale HLD problems, which are often computationally expensive. Bade and Bandyopadhyay [34] worked on a method to minimise the flow of a hot oil circuit between two plants. Although pumping and piping costs were not considered in the objective function, they were indirectly minimised by selecting the lowest possible hot oil flowrate.

HEN synthesis is a difficult problem to solve even for single plants [35]. When multiple plants and inter-plant heat integration are considered, it becomes even more challenging to obtain convergence. Song et al., combined the strengths of PA and MP in their work. In the first step, they divided the problem into smaller sections using an algorithm based on PA [36]. Then they carried out HEN synthesis of each section and finally optimised the inter-plant flows taking into account the pumping and piping costs [37]. Chang et al. [38] also proposed a method to simultaneously optimise the HEN and heat integration between plants. To simplify the problem, they considered a case with only two plants and using only a hot water loop to realise the heat exchange between them. The method was subsequently extended to more than two plants using different options (e.g., steam, hot oil) as intermediate fluids [39]. When a HEN is designed for more than one plant, it is important to determine the locations of the heat exchangers. Nair et al. [40] developed a MINLP method taking into account the locations of the heat exchangers in an eco-industrial park. They assumed that the temperature difference in the heat streams is linearly correlated to the travelled distance. They also considered piping and pumping costs and their trade-off with the operating cost benefits of heat recovery. Kachacha et al. [41] also considered the impact of plant location in the HEN problem by including piping and pumping costs. However, in order to keep the formulation linear, they made simplifying assumptions by using pre-calculated logarithmic mean temperature difference (LMTD) and pipe diameters. Laukkanen and Seppala [42] studied using nanofluids in inter-plant HEN synthesis. They developed a method to optimise the HEN, taking into account the trade-off between enhanced heat transfer and increased pumping power requirement due to the addition of nano-particles in the heat transfer fluid. Liu et al. [43] combined the efforts in mass integration and HEN synthesis in their heat integrated water allocation network model. Although they considered piping requirements for the water streams, they ignored heat losses and pumping requirements for transferring heat between the plants.

The literature of PI is rich in methods focused on inter-plant exchanges; however, graphical methods often neglect aspects related to plant layout. The most elaborate PA-based methods consider only heat integration using intermediate fluids and calculate heat losses and piping after integration. The MP methods address the location-based issues in inter-plant exchanges more extensively. However, most of the methods simplify the problem by considering the exchange only between two plants [38], identifying the excess heat manually [30] and optimising its valorisation instead of the overall system. Moreover, the integration of new utility systems was not a part of the optimisation [41], which might cause energy efficiency improvement opportunities to be missed. Another aspect overlooked in the literature is the type of the intermediate fluid which is used in inter-plant exchange. Methods have been specifically developed for heat sharing by steam [11], hot water [38] or hot oil [34]. Thus, the gaps in the literature are identified as:

1. not considering the simultaneous integration of energy conversion technologies and inter-plant heat and material exchange infrastructure,
2. only partially accounting for location aspects and
3. case-specific methods and lack of generalised applicability.

The work presented in this paper addresses such gaps by formulating the utility integration problem taking into account the location aspects. The method is generic and offers flexibility in integration of new technologies as well as infrastructure for inter-plant heat and material exchange and carries out their optimisation simultaneously.

3. Method

The method proposed in this work is a novel MILP formulation based on [44]. The unique aspect that this work introduces is the location of plants and distance between them to understand their impact on PI targets.

3.1. Definition of Main Sets

The basis of the method is modeling a system with mass and energy balances. The following mains sets are therefore defined:

- **TT**: The set of time steps to include the time-dependency of the system;
- **LC**: The set of plant locations in the optimisation problem;
- **U**: The set of units. Units are entities that represent an equipment (e.g., distillation column), a production unit or an entire plant, depending on its boundaries;
- **S**: The set of streams. Streams represent flows of energy or materials;
- **H**: The set of heat streams $\mathbf{H} \subset \mathbf{S}$. This set is used to create hot and cold streams;
- **Z**: The set of resource streams $\mathbf{Z} \subset \mathbf{S}$. This set is used to model material flows (e.g., water, natural gas);
- **ES**: The set of electricity streams $\mathbf{ES} \subset \mathbf{S}$. This set is used to model the electricity flows;
- **L**: The set of layers. Resource streams are assigned to a member (i.e., layer) in this set where the material is specified;

The problem is defined as a system which has time-dependent behaviour, to be able to capture different operating modes of plants in different time steps ($t \in \mathbf{TT}$). The locations ($lc \in \mathbf{LC}$) divide the system into smaller subsystems, in which the mass and energy balances are closed. The locations can exchange heat and resources with each other using only selected streams (i.e., inter-location streams) while electricity flows freely in the system, without location restrictions. In each location, there can be one or more units ($u \in \mathbf{U}$) that are characterised by streams ($s \in \mathbf{S}$). Streams can represent heat deficit (e.g., cold streams), heat excess (e.g., hot streams), resource deficit/excess and electricity deficit/excess.

Figure 1 depicts an illustrative example summarising the method. When a heat stream is used within a location it is not subject to heat losses. Conversely, heat losses apply to use the heat in

another location. Streams ($s \in \mathbf{S}$) which are used in a location different from their original one have a pressure drop associated to the transfer and a corresponding pumping requirement. The necessary infrastructure (i.e., piping) which must be installed to realise inter-location exchange is also considered in this work.

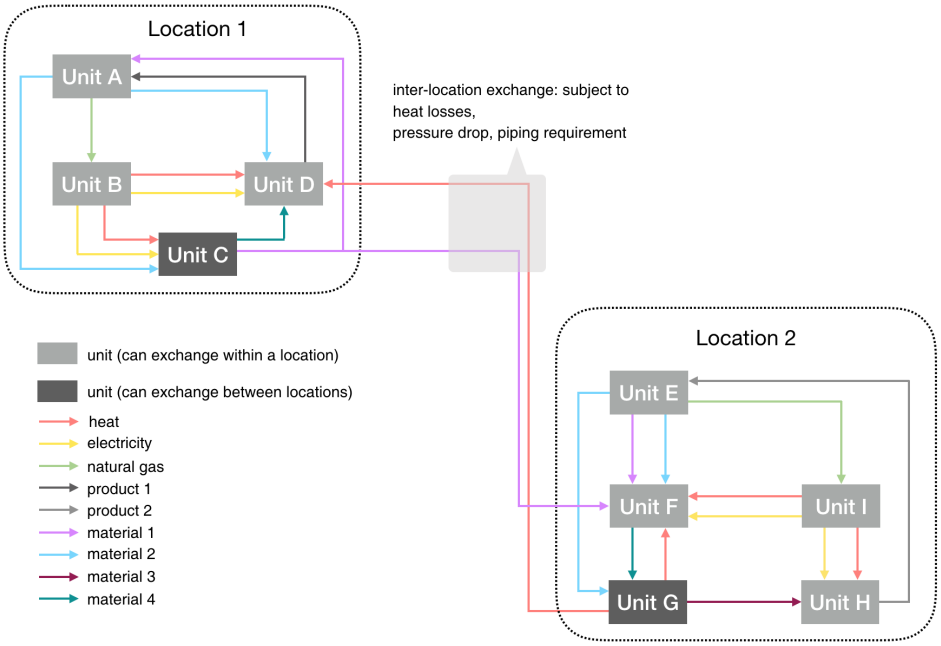

Figure 1. Simple graphical representation of the method.

3.2. Objective Function

Parametric optimisation is carried out with multiple objectives to generate and evaluate several scenarios. In MILP techniques used in PI, several objective functions are available in the literature. Economic objectives are the most applicable for this work, since the impact of distance can be monetised. Thus, the main objective (Equation (1)) is selected as the overall cost of the system excluding the investment in pipes for inter-location connections. The piping cost is selected as the second objective and integrated in the MILP framework as an ϵ-constraint (see Equation (2)).

$$\min \qquad C^{op} + C^{inv}, \tag{1}$$

$$C^{pipe} \leq \epsilon. \tag{2}$$

C^{op} represents the operating cost associated with the consumption of resources (Equation (3)) while C^{inv} is the annual investment cost for integrating new energy conversion technologies (Equation (4)) and C^{pipe} is the annualised investment cost for piping between locations.

$$C^{op} = \sum_{u \in \mathbf{U}} \left[\sum_{t \in \mathbf{TT}} \left(c_u^{op1} \cdot y'_{u,t} + c_u^{op2} \cdot f'_{u,t} \right) \cdot \Delta t_t^{op} \right], \tag{3}$$

$$C^{inv} = \left[\sum_{u \in \mathbf{U}} \left(c_u^{inv1} \cdot y_u + c_u^{inv2} \cdot f_u \right) \right] \cdot F^{an}, \tag{4}$$

where c_u^{op1} and c_u^{inv1} are the fixed operating and investment costs of the units associated with their activation, c_u^{op2} and c_u^{inv2} are the variable operating and investment costs of the units which depend on their size, Δt_t^{op} is the operating time and F^{an} is the annualisation factor based on interest rate and lifetime of the equipment.

3.3. Sizing and Scheduling

Sizing and scheduling constraints determine if units are used in a certain time step (i.e., scheduling) as well as the purchased capacity and the utilised capacity in each (i.e., sizing). The units can be divided in two categories based on their behaviour: process units ($pu \in \mathbf{PU} \subset \mathbf{U}$) and utility units ($uu \in \mathbf{UU} \subset \mathbf{U}$). Process units have fixed size and scheduling and represent the production units on industrial plants. The sizing and scheduling constraints for the process units are defined in Equations (5)–(8).

$$f'_{u,t} = 1 \quad \forall\, u \in \mathbf{PU},\ t \in \mathbf{TT}, \tag{5}$$

$$f_u = 1 \quad \forall\, u \in \mathbf{PU}, \tag{6}$$

$$y'_{u,t} = 1 \quad \forall\, u \in \mathbf{PU},\ t \in \mathbf{TT}, \tag{7}$$

$$y_u = 1 \quad \forall\, u \in \mathbf{PU}, \tag{8}$$

where f_u and $f'_{u,t}$ are the overall sizing factor and the sizing factor at time step $t \in \mathbf{TT}$ and y_u and $y'_{u,t}$ are binary variables which decide if a unit is purchased and utilised in time step $t \in \mathbf{TT}$, respectively. Hence although decision variables are defined for process units, they are eliminated by fixing their values.

Utility units are, defined with a certain size (i.e., reference size) but can be used in smaller and larger sizes as they scale with the sizing factor (f) according to the requirements of the process units. The equations governing the sizing and scheduling of utility units are Equations (9)–(12).

$$\mathrm{F}_u^{\min} \cdot y_u \leq f_u \leq \mathrm{F}_u^{\max} \cdot y_u \quad \forall\, u \in \mathbf{UU}, \tag{9}$$

$$f'_{u,t} \leq f_u \quad \forall\, u \in \mathbf{UU},\ t \in \mathbf{TT}, \tag{10}$$

$$\mathrm{F}_u^{\min} \cdot y'_{u,t} \leq f'_{u,t} \leq \mathrm{F}_u^{\max} \cdot y'_{u,t} \quad \forall\, u \in \mathbf{UU}, \tag{11}$$

$$y'_{u,t} \leq y_u \quad \forall\, u \in \mathbf{UU},\ t \in \mathbf{TT}, \tag{12}$$

where $\mathrm{F}_u^{\min}$ and $\mathrm{F}_u^{\max}$ are the lower and upper bounds of the sizing factor f_u respectively. More detail and explanations on the sizing and scheduling constraints can be found in [44].

3.4. Resource Balance and Links

The resource balance is closed for each layer in the overall system as well as in each location. Moreover, resource links are included to observe and limit the flow of resources between units. The following sets are defined for the resource balance constraints:

- $\mathbf{Z}_{u,l}$: This set consists of resource streams on layer $l \in \mathbf{L}$ in unit $u \in \mathbf{U}$;
- $\mathbf{U}_l$: The set of units of layer. This set consists of the units which have at least one resource stream on layer $l \in \mathbf{L}$;
- $\mathbf{U}_{lc}$: The set of units of location. This set comprises of the units in a given location $lc \in \mathbf{LC}$;
- $\mathbf{U}_{l,lc}$: The set of units of layer and location. This set includes the units in location $lc \in \mathbf{LC}$, which have at least one resource stream on layer $l \in \mathbf{L} \therefore \mathbf{U}_l \cap \mathbf{U}_{lc}$;
- $\mathbf{OL}_{lc}$: The set of other locations. For a given location $lc \in \mathbf{LC}$ this set includes all the other locations in the system $\therefore o \in \mathbf{OL}_{lc} : o \neq lc$;
- $\mathbf{OL}_u$: The set of other locations of a unit. For a given unit $u \in \mathbf{U}$ this set contains all the locations except for the original location of the unit. It is specifically useful for units which can transfer flows to other locations;
- $\mathbf{RL}_{l,u}$: The set of resource links of a unit. For a given layer $l \in \mathbf{L}$ and a unit of that layer $u \in \mathbf{U}_l$ this set consists of the other units on the same layer $\therefore i \in \mathbf{RL}_u : i \neq u$;

A unit can have several resource streams in the same layer; however, when the interactions of the units are considered, the flows in the same layer should be aggregated. This is enforced by Equation (13).

$$\dot{m}^{\text{in}}_{l,u,t} = \sum_{z \in \mathbf{Z}_{u,l}} \dot{m}^{\text{in}}_{l,z,t}, \quad \dot{m}^{\text{out}}_{l,u,t} = \sum_{z \in \mathbf{Z}_{u,l}} \dot{m}^{\text{out}}_{l,z,t} \quad \forall\, l \in \mathbf{L},\ u \in \mathbf{U}_l,\ t \in \mathbf{TT}, \tag{13}$$

where $\dot{m}^{\text{in}}_{l,u,t}$ and $\dot{m}^{\text{out}}_{l,u,t}$ are the in/out reference flows of unit $u \in \mathbf{U}$ and $\dot{m}^{\text{in}}_{l,r,t}$ and $\dot{m}^{\text{out}}_{l,r,t}$ are the inlet and outlet reference resource stream flows, respectively. Since the unit sizes vary depending on the scaling factor (f), the flows should also be scaled with respect to their units (see Equation (14)).

$$\dot{M}^{in}_{l,u,t} = \dot{m}^{\text{in}}_{l,u,t} \cdot f'_{u,t}, \quad \dot{M}^{out}_{l,u,t} = \dot{m}^{\text{out}}_{l,u,t} \cdot f'_{u,t} \quad \forall\, l \in \mathbf{L},\ u \in \mathbf{U}_l,\ t \in \mathbf{TT}, \tag{14}$$

where $\dot{M}^{in}_{l,u,t}$ and $\dot{M}^{out}_{l,u,t}$ are scaled flows into/out of the unit, respectively. The overall resource balance (see Equation (15)) is included such that resource requirements of the units in the system are fulfilled by the other units.

$$\sum_{u \in \mathbf{U}_l} \dot{M}^{in}_{l,u,t} = \sum_{u \in \mathbf{U}_l} \dot{M}^{out}_{l,u,t} \quad \forall\, l \in \mathbf{L},\ t \in \mathbf{TT}. \tag{15}$$

The resource flow from each unit $\mathbf{U}_l$ is transferred to the other units $i \in \mathbf{RL}_{l,u}$ in the system via resource links. Similarly, the total resource flow into a unit is the sum of the flows from the units $j \in \mathbf{RL}_{l,u}$ in the resource links. These two conditions are combined in a single constraint (Equation (16)). The resource flow from a unit to the others is limited to its outflow. This constraint is imposed by Equation (17)

$$\dot{M}^{out}_{l,u,t} + \sum_{i \in \mathbf{RL}_{l,u}} \dot{M}^{rl}_{l,i,u,t} = \dot{M}^{in}_{l,u,t} + \sum_{j \in \mathbf{RL}_{l,u}} \dot{M}^{rl}_{l,u,j,t} \quad \forall\, l \in \mathbf{L},\ u \in \mathbf{U}_l,\ t \in \mathbf{TT}, \tag{16}$$

$$\sum_{j \in \mathbf{RL}_{l,u}} \dot{M}^{rl}_{l,u,j,t} \le \dot{M}^{out}_{l,u,t} \quad \forall\, l \in \mathbf{L},\ u \in \mathbf{U}_l,\ t \in \mathbf{TT}, \tag{17}$$

where $\dot{M}^{rl}_{l,i,u,t}$ and $\dot{M}^{rl}_{l,u,j,t}$ are positive continuous variables which represent the flows in layer $l \in \mathbf{L}$ from unit $i \in \mathbf{RL}_u$ to $u \in \mathbf{U}_l$ and from $u \in \mathbf{U}_l$ to $j \in \mathbf{RL}_u$, respectively. Some units can exchange resources only within their origin location while others can have inter-location resource transfer. For units with inter-location resource exchange, a split factor is defined to determine the magnitude of the resource flow transferred to the other locations as seen in Equation (18).

$$\sum_{i \in \mathbf{U}_{l,o}} \dot{M}^{rl}_{l,i,u,t} = \dot{m}^{\text{out}}_{l,u,t} \cdot a_{l,lc,o,u,t} \quad \forall\, l \in \mathbf{L},\ lc \in \mathbf{LC},\ o \in \mathbf{OL}_{lc},\ u \in \mathbf{U}_l,\ t \in \mathbf{TT}, \tag{18}$$

where $a_{l,lc,o,u,t}$ is the split factor of the flow in layer $l \in L$ in unit $u \in \mathbf{U}_l$ from location $lc \in \mathbf{LC}$ to the other locations $o \in \mathbf{OL}_{lc}$. The resource balance is closed within locations as well as for the overall system. For a given location $lc \in \mathbf{LC}$ and layer $l \in \mathbf{L}$, the supply flows are those from the units of that location $u \in \mathbf{U}_{l,lc}$ and inter-location flows from the other locations. Similarly, the demand flows are those to the units of that location $u \in \mathbf{U}_{l,lc}$ and the inter-location flows to the other locations. Equation (19) ensures that the supply flow in a location is equal to the demand.

$$\begin{aligned} &\textstyle\sum_{o \in \mathbf{OL}_{lc}} \sum_{u \in \mathbf{U}_{l,o}} \dot{m}^{\text{out}}_{l,u,t} \cdot a_{l,o,lc,u,t} + \sum_{u \in \mathbf{U}_{l,lc}} \dot{M}^{out}_{l,u,t} \\ &= \textstyle\sum_{o \in \mathbf{OL}_{lc}} \sum_{u \in \mathbf{U}_{l,o}} \dot{m}^{\text{out}}_{l,u,t} \cdot a_{l,lc,o,u,t} + \sum_{u \in \mathbf{U}_{l,lc}} \dot{M}^{in}_{l,u,t} \quad \forall\, l \in \mathbf{L},\ lc \in \mathbf{LC},\ t \in \mathbf{TT}. \end{aligned} \tag{19}$$

3.5. Distribution Heat Losses

Direct heat exchange between process streams has been considered as an option for heat recovery in several case studies [45]; however, its drawbacks have also been highlighted [11]. Especially when sharing heat over long distances, direct exchange between process streams becomes impractical. Therefore, the distribution of heat between locations is carried out by using intermediate heat transfer media (e.g., hot water, steam, etc.).

Conceptually, heat streams that are allowed to exchange between locations are first duplicated and assigned to the other locations in the system. All duplicates as well as the stream itself are then assigned to a stream parent. Stream parents, although possessing no physical correspondence, are entities used to group the streams with their duplicates in different locations. There are two options for the heat streams that could be shared between different locations; to use them in their original location or to use their duplicate in other locations. These actions can be taken mutually; a stream can be used in its original location while its duplicate is used in another location. When the heat streams are used in the location of origin, it is assumed that heat losses do not occur, while heat losses and temperature drop apply for their duplicates in other locations. This is illustrated in Figure 2 considering heat distribution by steam and hot water as examples.

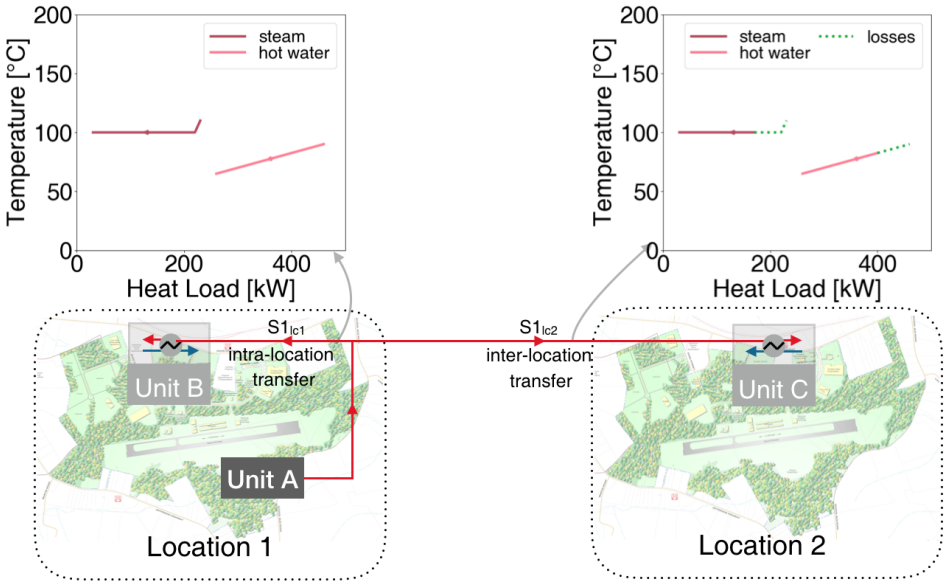

Figure 2. Distribution heat losses and their impact on the temperature-enthalpy profile.

In order to transfer heat between locations, pipes should be installed. To transport the fluid in urban areas, underground pipes are preferable because of regulations, but in other settings, above-ground pipes could be a better option since they have lower investment cost. However, as ground acts like an additional layer of insulation, heat losses in underground transfers are lower. Since both options are considered, another layer of decision is introduced in the problem, by creating duplicates of the streams for different transfer types (i.e., underground and above-ground). Heat losses in each transfer type are calculated following the methods explained in Sections 3.5.1 and 3.5.2. Considering the temperature drop associated with the heat losses, the temperature-heat profiles of the duplicate streams are reconstructed.

3.5.1. Above-Ground Heat Losses

Heat losses in above-ground pipes occur because of heat transfer to ambient air. Assuming that the inner surface of the pipes is at the same temperature as the fluid flowing through them, the calculation

of the heat losses can be simplified. The overall heat transfer coefficient and the surface area of the heat distribution pipes are calculated using Equations (20) and (21).

$$\frac{1}{V_s} = \frac{1}{h^{amb}} + \frac{x_s^{pipe}}{\lambda_s^{pipe}} + \frac{x_s^{ins}}{\lambda_s^{ins}} \quad \forall\, s \in \mathbf{H}, \tag{20}$$

$$A_{s,lc,o}^{pipe} = 2 \cdot \pi \cdot d_s^{ins} \cdot l_{lc,o}^{pipe} \quad \forall\, s \in \mathbf{H},\ lc \in \mathbf{LC},\ o \in \mathbf{OL}_{lc}, \tag{21}$$

where V_s is overall heat transfer coefficient, h^{amb} is the convective heat transfer coefficient of ambient air, λ_s^{pipe} and λ_s^{ins} are the conductive heat transfer coefficients of pipe and insulation, x_s^{pipe} and x_s^{ins} are the thickness of the pipe and of the insulation material, $l_{lc,o}^{pipe}$, d_s^{ins} and $A_{s,lc,o}^{pipe}$ are the length, insulated diameter and surface area of the pipe, respectively. The heat losses in the supply and return are then calculated using simple heat transfer equations (Equations (22) and (23)) and the remaining heat content of the stream is obtained by subtracting the distribution losses (Equation (24)).

$$\dot{q}_{s,lc,o,t}^{sup} = V_s \cdot A_{s,lc,o}^{pipe} \cdot \left(T_{s,t}^{in'} - T_t^{amb}\right) \quad \forall\, s \in \mathbf{H},\ lc \in \mathbf{LC},\ o \in \mathbf{OL}_{lc},\ t \in \mathbf{TT}, \tag{22}$$

$$\dot{q}_{s,lc,o,t}^{ret} = V_s \cdot A_{s,lc,o}^{pipe} \cdot \left(T_{s,t}^{out'} - T_t^{amb}\right) \quad \forall\, s \in \mathbf{H},\ lc \in \mathbf{LC},\ o \in \mathbf{OL}_{lc},\ t \in \mathbf{TT}, \tag{23}$$

$$\dot{q}_{s,t} = \dot{q}'_{s,t} - \dot{q}_{s,lc,o,t}^{sup} - \dot{q}_{s,lc,o,t}^{ret} \quad \forall\, s \in \mathbf{H},\ lc \in \mathbf{LC},\ o \in \mathbf{OL}_{lc},\ t \in \mathbf{TT}, \tag{24}$$

where $\dot{q}_{s,lc,o,t}^{sup}$ and $\dot{q}_{s,lc,o,t}^{ret}$ are the heat losses at supply and return, $T_{s,t}^{in'}$ and $T_{s,t}^{out'}$ are the inlet and the exit temperatures of the stream prior to heat losses, $\dot{q}'_{s,t}$ and $\dot{q}_{s,t}$ are the heat content of the stream prior to and after the heat losses and T_t^{amb} is the ambient temperature.

3.5.2. Underground Heat Losses

The heat loss calculations for heat distribution with underground pipes is adapted from [46]. To simplify the problem, convection at the surface of the ground is converted to an equivalent layer of soil and added to the depth by Equation (25).

$$x^{ground} = x^{ground'} + \frac{\lambda^{ground}}{h^{amb}}, \tag{25}$$

where λ^{ground} is the conductive heat transfer coefficient of ground, $x^{ground'}$ is the real pipe depth and x^{ground} is the corrected pipe depth (i.e., thickness of soil). Heat losses also depend on the thermal resistance. In the case of heat distribution with double pipes (i.e., supply and return) the thermal resistance comes from the mutual interaction of the pipes, the ground and the insulation material. These parameters are calculated according to Equations (26)–(28).

$$X_s^{mut} = \frac{1}{4 \cdot \pi \cdot \lambda^{ground}} \cdot \ln\left[1 + \left(\frac{2 \cdot x^{ground}}{l^{pp}}\right)^2\right] \quad \forall\, s \in \mathbf{H}, \tag{26}$$

$$X_s^{ground} = \frac{1}{2 \cdot \pi \cdot \lambda^{ground}} \cdot \ln\left(\frac{4 \cdot x^{ground}}{D_s^{ins}}\right) \quad \forall\, s \in \mathbf{H}, \tag{27}$$

$$X_s^{ins} = \frac{1}{2 \cdot \pi \cdot \lambda_s^{ins}} \cdot \ln\left(\frac{D_s^{ins}}{D_s^{pipe}}\right) \quad \forall\, s \in \mathbf{H}, \tag{28}$$

where l^{pp} is the distance between the supply and return pipes, D_s^{pipe} is the diameter of the pipe excluding the insulation and X_s^{mut}, X_s^{ground} and X_s^{ins} are the thermal resistances of the mutual

interaction between the pipes, ground and insulation material, respectively. The heat loss coefficients $W_s^{'}$ and $W_s^{''}$ are then calculated using Equation (29).

$$W_s^{'} = \frac{X_s^{\text{ground}} + X_s^{\text{ins}}}{\left(X_s^{\text{ground}} + X_s^{\text{ins}}\right)^2 - X_s^{\text{mut}2}} \quad W_s^{''} = \frac{X_s^{\text{mut}} + X_s^{\text{ins}}}{\left(X_s^{\text{ground}} + X_s^{\text{ins}}\right)^2 - X_s^{\text{mut}2}} \quad \forall\, s \in \mathbf{H}. \tag{29}$$

The heat losses at supply and return are calculated using Equations (30) and (31) and are subtracted from the heat load of the stream (see Equation (24))

$$\dot{q}_{s,lc,o,t}^{\text{sup}} = \left[\left(W_s^{'} - W_s^{''}\right) \cdot \left(T_{s,t}^{\text{in}} - T_t^{\text{ground}}\right) + W_s^{''} \cdot \left(T_{s,t}^{\text{in}} - T_{s,t}^{\text{out}}\right)\right] \cdot l_{lc,o}^{\text{pipe}} \quad \forall\, s \in \mathbf{H}, \; lc \in \mathbf{LC},\; o \in \mathbf{OL}_{lc},\; t \in \mathbf{TT}, \tag{30}$$

$$\dot{q}_{s,lc,o,t}^{\text{ret}} = \left[\left(W_s^{'} - W_s^{''}\right) \cdot \left(T_{s,t}^{\text{out}} - T_t^{\text{amb}}\right) - W_s^{''} \cdot \left(T_{s,t}^{\text{in}} - T_{s,t}^{\text{out}}\right)\right] \cdot l_{lc,o}^{\text{pipe}} \quad \forall\, s \in \mathbf{H}, \; lc \in \mathbf{LC},\; o \in \mathbf{OL}_{lc},\; t \in \mathbf{TT}. \tag{31}$$

3.5.3. Modified Heat Cascade

The heat cascade constraints close the heat balance and make sure that heat flows from higher to lower temperatures. In the state-of-the-art targeting formulation [44], the heat balance is closed for the overall system. However, in this work with the introduction of locations, it is closed for each location, including the streams that can exchange between locations. The heat cascade set and parameter definitions are listed as follows:

- $\mathbf{K}_{lc}$: The set of temperature intervals of a location. An interval represents the zone above a certain temperature level (T_k^{lb}). Thus, this set is formed of intervals created by unique temperatures in each location in ascending order;
- T_k^{lb}: Temperature level of the interval $k \in \mathbf{K}_{lc}$. This parameter sets the lower bound of the interval;
- $\mathbf{HS}_{lc}$: The set of hot streams in each location ($lc \in \mathbf{LC}$). It includes the streams that are originally in the location as well as the inter-location streams from the other locations;
- $\mathbf{CS}_{lc}$: The set of cold streams in each location ($lc \in \mathbf{LC}$). It includes the streams that are originally in the location as well as the inter-location streams from the other locations;
- $\mathbf{HS}_{lc,k}$: The set of hot streams in each location ($lc \in \mathbf{LC}$) and temperature interval ($k \in \mathbf{K}$) $\therefore \mathbf{HS}_{lc,k} \in \mathbf{HS}_{lc}$. A hot stream $i \in \mathbf{HS}_{lc}$ is in a certain interval if its inlet temperature is higher than the temperature level of the interval $\therefore T_{i,t}^{\text{in}} \geq T_k^{\text{lb}}$
- $\mathbf{CS}_{lc,k}$: The set of cold streams in each location ($lc \in \mathbf{LC}$) and temperature intervals ($k \in \mathbf{K}$) $\therefore \mathbf{CS}_{lc,k} \in \mathbf{CS}_{lc}$. A cold stream $j \in \mathbf{CS}_{lc}$ is in a certain interval if its outlet temperature is higher than the temperature level of the interval $\therefore T_{j,t}^{\text{out}} \geq T_k^{\text{lb}}$
- $\mathbf{HI}$: The set of heat streams that are allowed to transfer heat between locations (i.e., inter-location streams) $\therefore \mathbf{HI} \subset \mathbf{H}$;
- $\mathbf{HI}_u$: The set of inter-location heat streams in unit $u \in \mathbf{U}$ $\therefore \mathbf{HI}_u \subset \mathbf{HI}$
- $\mathbf{P}$: The set of heat stream parents. When a stream is allowed to be used in different locations (i.e., $\therefore s \in \mathbf{HI}$), it is duplicated in other locations as explained in Section 3.5. Parents are used to assign a stream and its duplicates to the same entity;
- $\mathbf{P}_u$: The set of stream parents of a unit $\therefore \mathbf{P}_u \subset \mathbf{P}$;
- $\mathbf{H}_u$: The set of heat streams of a unit $\therefore \mathbf{H}_u \subset \mathbf{H}$;
- $\mathbf{S}_p$: The set of streams of parents. Streams and their duplicates in other locations are aggregated in this set;
- $\mathbf{OL}_p$: Other locations of a parent. This set contains all the locations in the problem except for the original location of the parent;

- **TR**: The set of transfer types. The elements of this set are predefined as 'under-ground' and 'above-ground' since those are the transfer types considered for heat streams;
- $\mathbf{S}_{p,lc,tr}$: The set of streams of parents in each location and for each transfer type $\therefore \mathbf{S}_{p,lc,tr} \subset \mathbf{HI}$;

In order to be able to calculate the heat loads of the streams in the temperature intervals, their heat capacities are calculated according to Equation (32).

$$\dot{m}c_{P_{s,t}} = \frac{\dot{q}_{s,t}}{|T^{in}_{s,t} - T^{out}_{s,t}|} \quad \forall\, s \in \mathbf{H},\ t \in \mathbf{TT}, \tag{32}$$

where $\dot{q}_{s,t}$ is the total reference heat load of the stream, $T^{in}_{s,t}$ is the inlet temperature, $T^{out}_{s,t}$ is the outlet temperature and $\dot{m}c_{P_{s,t}}$ is the heat capacity. In each interval, heat either flows from hot streams to the cold streams or is transferred to other intervals in the form of residual heat. This is enforced by Equation (33).

$$\Big(\sum_{h \in \mathbf{HS}_{lc,k}} \dot{q}_{h,k,t} \cdot s_{h,t}\Big) - \Big(\sum_{c \in \mathbf{CS}_{lc,k}} \dot{q}_{c,k,t} \cdot s_{c,t}\Big) - \dot{R}_{lc,k,t} = 0 \quad \forall\, lc \in \mathbf{LC},\ k \in \mathbf{K}_{lc},\ t \in \mathbf{TT}, \tag{33}$$

where $\dot{R}_{lc,k,t}$ is the continuous positive variable representing the residual heat in the interval, $\dot{q}_{h,k,t}$ and $\dot{q}_{c,k,t}$ are the reference heat loads of hot and cold streams in interval k, respectively, and $s_{h,t}$ and $s_{c,t}$ are scaling factors of the hot and cold streams, respectively. The reference load of a stream in an interval is equal to its total reference load if it is fully in the interval (Equations (34) and (35)). Otherwise the partial load of the stream in the interval is calculated (Equations (36) and (37)).

$$\dot{q}_{h,k,t} = \dot{m}c_{Ph,t} \cdot \left(T^{in}_{h,t} - T^{out}_{h,t}\right) \quad \forall\, h \in \mathbf{HS}_{lc,k},\ lc \in \mathbf{LC},\ k \in \mathbf{K}_{lc},\ t \in \mathbf{TT}, \tag{34}$$

$$\dot{q}_{c,k,t} = \dot{m}c_{Pc,t} \cdot \left(T^{out}_{c,t} - T^{in}_{c,t}\right) \quad \forall\, c \in \mathbf{CS}_{lc,k},\ lc \in \mathbf{LC},\ k \in \mathbf{K}_{lc},\ t \in \mathbf{TT}, \tag{35}$$

$$\dot{q}_{h,k,t} = \dot{m}c_{Ph,t} \cdot \left(T^{in}_{h,t} - T^{1}_{k}\right) \quad \forall\, h \in \mathbf{HS}_{lc,k},\ lc \in \mathbf{LC},\ k \in \mathbf{K}_{lc},\ t \in \mathbf{TT}, \tag{36}$$

$$\dot{q}_{c,k,t} = \dot{m}c_{Pc,t} \cdot \left(T^{out}_{c,t} - T^{1}_{k}\right) \quad \forall\, c \in \mathbf{CS}_{lc,k},\ lc \in \mathbf{LC},\ k \in \mathbf{K}_{lc},\ t \in \mathbf{TT}. \tag{37}$$

Abiding by the first law of thermodynamics, since energy cannot be created or destroyed, residual heat at the top and bottom intervals are set to zero (Equation (38)).

$$\dot{R}_{lc,k,t} = 0 \quad \forall\, lc \in \mathbf{LC}, t \in \mathbf{TT}, k = first(\mathbf{K}_{lc})\ or\ k = last(\mathbf{K}_{lc}). \tag{38}$$

The flow of a stream is scaled with its associated unit; hence, the scaling factor of a heat stream is equal to that of its unit (see Equation (39)). However, this applies only to the streams which cannot exchange between locations.

$$f'_{u,t} = s_{s,t} \quad \forall\, u \in \mathbf{U},\ s \in \mathbf{H}_u,\ t \in \mathbf{TT} :\ s \notin \mathbf{HI}. \tag{39}$$

For the inter-location streams, splitting is taken into account using stream parents ($p \in \mathbf{P}$). A parent of an inter-location stream can be used in its original location as well as other locations. In addition, it can be transferred between locations using different transfer types ($tr \in \mathbf{TR}$). The sum of all splitting factors of a parent is equal to the scaling factor of its unit. This is enforced by Equation (40).

$$f'_{u,t} = \sum_{lc \in \mathbf{LC}} \sum_{tr \in \mathbf{TR}} b_{p,t,lc,tr} \quad \forall\, u \in \mathbf{U},\ p \in \mathbf{P}_u,\ t \in \mathbf{TT}, \tag{40}$$

where $b_{p,t,lc,tr}$ is the splitting factor of parents in each location, time and for different transfer types. Similar to the relationship between units and streams, the streams of a parent scale together with the parent (Equation (41)).

$$s_{s,t} = b_{p,t,lc,tr} \quad \forall\, p \in \mathbf{P},\ t \in \mathbf{TT},\ lc \in \mathbf{LC},\ tr \in \mathbf{TR},\ s \in \mathbf{S}_{p,lc,tr}. \tag{41}$$

3.6. Distribution Pump Work

Heat and resource flows between locations are subject to pressure drop, which must be compensated by pumping. The pumping power requirement for inter-location exchange is considered by including additional electricity demand in the problem. The friction factor must be calculated first to estimate the pressure drop. Instead of the generic Colebrook equation, an explicit approximation by Haaland [47] is used in this work (see Equation (42)) as suggested by [48]. The Reynolds number is calculated using stream properties and pipe geometry, according to Equation (43).

$$\mathrm{ff}_{s,t} = \left\{ -1.8 \cdot \log_{10}\left[\left(\frac{\varepsilon_s}{3.7} \right)^{1.11} + \frac{6.9}{\mathrm{Re}_{s,t}} \right] \right\}^{-2} \quad \forall\, s \in \mathbf{S},\ t \in \mathbf{TT}, \tag{42}$$

$$\mathrm{Re}_{s,t} = \frac{\mathrm{u}_s \cdot \mathrm{d}_s}{\nu_{s,t}} \quad \forall\, s \in \mathbf{S},\ t \in \mathbf{TT}, \tag{43}$$

where $\nu_{s,t}$ is the kinematic viscosity, u_s is the velocity, $\mathrm{Re}_{s,t}$ is the Reynold's number, ε_s is the pipe roughness and $\mathrm{ff}_{s,t}$ is the friction factor. The pressure drop is then calculated using the Darcy-Weisbach equation, Equation (44).

$$\Delta \mathrm{P}_{s,t,lc,o} = \mathrm{ff}_{s,t} \cdot \left(\frac{\mathrm{l}_{lc,o}^{\mathrm{pipe}}}{\mathrm{d}_s^{\mathrm{pipe}}} \right) \cdot \left(\frac{\rho_{s,t}}{2} \right) \cdot {\mathrm{u}_{s,t}}^2 \quad \forall\, s \in \mathbf{S},\ t \in \mathbf{TT},\ lc \in \mathbf{LC},\ o \in \mathbf{OL}_{lc}, \tag{44}$$

where $\rho_{s,t}$ represents the density and $\Delta \mathrm{P}_{s,t,lc,o}$ the pressure drop. Ignoring the mechanical inefficiencies of pumps, the required electricity to drive them is calculated by Equation (45).

$$\dot{\mathrm{e}}_{s,t,lc,o}^{\mathrm{pm}} = \Delta \mathrm{P}_{s,t,lc,o} \cdot \mathrm{u}_{s,t} \cdot \frac{\pi \cdot \mathrm{d}_s^{\mathrm{pipe}^2}}{4} \quad \forall\, s \in \mathbf{S},\ t \in \mathbf{TT},\ lc \in \mathbf{LC},\ o \in \mathbf{OL}_{lc}, \tag{45}$$

where $\dot{\mathrm{e}}_{s,t,lc,o}^{\mathrm{pm}}$ is the reference pumping electricity requirements for the transfer of a stream between two locations. Resource streams require a transfer in only one direction since they are consumed at the target location. On the other hand, heat streams require bi-directional transfer because they have supply and return pipes. Thus, for heat streams, the pumping requirement is the sum of the electricity required in the supply and return pipes (see Equation (46)).

$$\dot{\mathrm{e}}_{s,t,lc,o}^{\mathrm{pm}} = \dot{\mathrm{e}}_{s,t,lc,o}^{\mathrm{sup}} + \dot{\mathrm{e}}_{s,t,lc,o}^{\mathrm{ret}} \quad \forall\, s \in \mathbf{H},\ t \in \mathbf{TT},\ lc \in \mathbf{LC},\ o \in \mathbf{OL}_{lc}, \tag{46}$$

where $\dot{\mathrm{e}}_{s,t,lc,o}^{\mathrm{sup}}$ and $\dot{\mathrm{e}}_{s,t,lc,o}^{\mathrm{ret}}$ are the reference pumping power requirement at the supply and return respectively. It should be noted that the parameter $\dot{\mathrm{e}}_{s,t,lc,o}^{\mathrm{pm}}$ corresponds to a certain flow (e.g., reference flow). Hence, the pumping requirement of a flow scales with it. This is carried out for the resource (Equation (47)) and heat (Equation (48)) streams in two separate equations since different scaling factors are defined for different types of streams.

$$\dot{E}_{s,t,o}^{pm} = \dot{\mathrm{e}}_{s,t,lc,o}^{\mathrm{pm}} \cdot a_{l,lc,o,u,t} \quad \forall\, l \in \mathbf{L},\ u \in \mathbf{U}_{lc},\ t \in \mathbf{TT},\ lc \in \mathbf{LC},\ o \in \mathbf{OL}_{lc}, s \in \mathbf{Z}_{u,l}, \tag{47}$$

$$\dot{E}_{s,t,o}^{pm} = \dot{\mathrm{e}}_{s,t,lc,o}^{\mathrm{pm}} \cdot b_{p,t,o,tr} \quad \forall\, p \in \mathbf{P},\ t \in \mathbf{TT},\ lc \in \mathbf{LC},\ o \in \mathbf{OL}_{lc},\ s \in \mathbf{S}_{p,lc,tr}, \tag{48}$$

where $\dot{E}_{s,t,o}^{pm}$ is the pumping electricity requirement

3.7. Electricity Balance

Contrary to resource and heat streams, location restrictions do not apply to the electricity streams since the losses and infrastructure investment in the transfer of electricity are negligible compared to the others. To define the electricity balance, the following set is defined:

- $\mathbf{ES}_u$: This set consists of electricity streams in unit $u \in \mathbf{U}$;

Similar to resource streams, there might be several electricity streams in a unit. The reference flows of electricity in and out of a unit are calculated as the sum its electricity streams by Equation (49).

$$\dot{e}^{\text{in}}_{u,t} = \sum_{es \in \mathbf{ES}_u} \dot{e}^{\text{in}}_{es,t}, \quad \dot{e}^{\text{out}}_{u,t} = \sum_{es \in \mathbf{ES}_u} \dot{e}^{\text{out}}_{es,t} \quad \forall\, u \in \mathbf{U},\ t \in \mathbf{TT}, \tag{49}$$

where $\dot{e}^{\text{in}}_{u,t}$ is the reference inflow and $\dot{e}^{\text{out}}_{u,t}$ is the reference outflow of electricity of unit $u \in \mathbf{U}$. The electricity flows of a unit, like other flows, scale with the unit itself. To obtain the real electricity generation/demand of a unit, the scaling factor is taken into account in Equations (50) and (51). In addition to the electricity streams, the demand of a unit includes the electricity for pumping resources and heat to other locations which is included in Equation (51).

$$\dot{E}^{out}_{u,t} = \dot{e}^{\text{out}}_{u,t} \cdot f'_{u,t} \quad \forall\, u \in \mathbf{U},\ t \in \mathbf{TT}, \tag{50}$$

$$\dot{E}^{in}_{u,t} = \dot{e}^{\text{in}}_{u,t} \cdot f'_{u,t} + \Big(\sum_{o \in \mathbf{OL}_{lc}} \sum_{s \in \mathbf{HI}_u} \dot{E}^{pm}_{s,t,o} \Big) + \Big(\sum_{o \in \mathbf{OL}_{lc}} \sum_{l \in \mathbf{L}} \sum_{s \in \mathbf{Z}_{u,l}} \dot{E}^{pm}_{s,t,o} \Big) \quad \forall\, lc \in \mathbf{LC},\ u \in \mathbf{U}_{lc},\ t \in \mathbf{TT}, \tag{51}$$

where $\dot{E}^{out}_{u,t}$ and $\dot{E}^{in}_{u,t}$ are positive continuous variables representing the electricity supply and demand of the units, respectively. Finally, electricity demand of the units in the system is satisfied by the other units, which is imposed by Equation (52)

$$\sum_{u \in \mathbf{U}} \dot{E}^{in}_{u,t} = \sum_{u \in \mathbf{U}} \dot{E}^{out}_{u,t} \quad \forall\, t \in \mathbf{TT}. \tag{52}$$

3.8. Distribution Piping Cost

To realise heat and resource sharing between locations, the necessary infrastructure (i.e., pipeline) must be installed. Neglecting the investment for piping would result in unrealistically optimistic scenarios; therefore, this work includes the piping cost in the formulation. In multi-time problems, the flow of heat and resources between locations might vary in different time steps. The installed pipes must be capable of handling the flows at any time step; hence, the sizing of the pipes is carried out with respect to the maximum flow over all time steps (see Equations (53) and (54)).

$$\dot{Q}^{max}_{p,o,tr} = \max(\dot{q}_{s,t} \cdot b_{p,t,o,tr}) \quad \forall\, p \in \mathbf{P}, t \in \mathbf{TT}, s \in \mathbf{S}_p, o \in \mathbf{OL}_p, tr \in \mathbf{TR}_p, \tag{53}$$

$$\dot{M}^{max}_{l,o,u} = \max(\dot{m}^{\text{out}}_{l,u,t} \cdot a_{l,lc,o,u,t}) \quad \forall\, l \in \mathbf{L},\ lc \in \mathbf{LC},\ o \in \mathbf{OL}_{lc},\ u \in \mathbf{U}_l,\ t \in \mathbf{TT}. \tag{54}$$

The max function is non-linear but can be converted to a set of linear constraints by introducing new continuous and binary variables. Linearisation of $\dot{Q}^{max}_{p,o,tr}$ is shown in Equations (55)–(60). A similar procedure is applied to linearise $\dot{M}^{max}_{l,o,u}$ but the equations are not included here.

$$\dot{q}_{s,t} \cdot b_{p,t,o,tr} \leq \dot{Q}^{max}_{p,o,tr} \quad \forall\, p \in \mathbf{P},\ t \in \mathbf{TT},\ s \in \mathbf{S}_p,\ o \in \mathbf{OL}_p,\ tr \in \mathbf{TR}, \tag{55}$$

$$\dot{G}_{p,t,o,tr} \leq \dot{q}_{s,t} \cdot b_{p,t,o,tr} \quad \forall\, p \in \mathbf{P},\ t \in \mathbf{TT},\ s \in \mathbf{S}_p,\ o \in \mathbf{OL}_p,\ tr \in \mathbf{TR}, \tag{56}$$

$$\dot{q}_{s,t} \cdot b_{p,t,o,tr} - \Big(1 - w_{p,t,o,tr}\Big) \cdot \text{bigM} \leq \dot{G}_{p,t,o,tr} \quad \forall\, p \in \mathbf{P},\ t \in \mathbf{TT},\ s \in \mathbf{S}_p,\ o \in \mathbf{OL}_p,\ tr \in \mathbf{TR}, \tag{57}$$

$$\dot{Q}^{max}_{p,o,tr} \leq \dot{G}_{p,t,o,tr} + \Big(1 - w_{p,t,o,tr}\Big) \cdot \text{bigM} \quad \forall\, p \in \mathbf{P},\ t \in \mathbf{TT},\ o \in \mathbf{OL}_p,\ tr \in \mathbf{TR}, \tag{58}$$

$$\dot{G}_{p,t,o,tr} \leq w_{p,t,o,tr} \cdot \text{bigM} \quad \forall\ p \in \mathbf{P},\ t \in \mathbf{TT},\ o \in \mathbf{OL}_p,\ tr \in \mathbf{TR}, \tag{59}$$

$$\sum_{t \in \mathbf{TT}} w_{p,t,o,tr} = 1 \quad \forall\ p \in \mathbf{P},\ t \in \mathbf{TT},\ o \in \mathbf{OL}_p,\ tr \in \mathbf{TR}, \tag{60}$$

where $\dot{Q}^{max}_{p,o,tr}$ is the maximum heat load of a stream parent per location and transfer type over time steps, $\dot{G}_{p,t,o,tr}$ is a slack variable which takes the value of $\dot{q}_{s,t} \cdot b_{p,t,o,tr}$ at the time step of the maximal load and 0 in the other time steps, $w_{p,t,o,tr}$ is a binary variable which takes the value of 1 at the time step of maximal load and 0 in other time steps and bigM is a large number for the big-M constraints [49].

Piping cost can be considered as a discrete function of the pipe diameter since there are standard pipe diameters and specific costs associated to them [50]. Such a relationship (see Table 1) is obtained by taking the average of the piping cost functions available in [51–54]. This relationship can be converted to flow-cost relationships using the stream properties.

Table 1. Piping cost for standard piping diameters.

Standard pipe size	1	2	3	4	5	6	7	8	9	10	11	12
Diameter [mm]	20	40	65	80	100	125	150	200	250	300	400	450
Specific cost [€/m]	96	166	250	312	387	480	580	775	975	1180	1588	1797

Each standard pipe size ($ps \in \mathbf{PS}$) has an upper bound ($\dot{q}^{ub}_{p,o,tr,ps}$ or $\dot{m}^{ub}_{l,u,o,ps}$) representing the maximum heat/mass that can flow through it as well as a lower bound ($\dot{q}^{lb}_{p,o,tr,ps}$ or $\dot{m}^{lb}_{l,u,o,ps}$). A new binary variable and a set of constraints are defined to determine the standard pipe size required for the flows. The constraints for the heat flow pipes are given in Equations (61)–(63).

$$\dot{q}^{lb}_{p,o,tr,ps} \cdot n^{h}_{p,o,tr,ps} \leq \dot{I}^{p}_{p,o,tr,ps} \leq \dot{q}^{ub}_{p,o,tr,ps} \cdot n^{h}_{p,o,tr,ps} \quad \forall\ p \in \mathbf{P},\ o \in \mathbf{OL}_p,\ tr \in \mathbf{TR},\ ps \in \mathbf{PS}, \tag{61}$$

$$\sum_{ps \in \mathbf{PS}} \dot{I}^{p}_{p,o,tr,ps} = \dot{Q}^{max}_{p,o,tr} \quad \forall\ p \in \mathbf{P},\ o \in \mathbf{OL}_p,\ tr \in \mathbf{TR},\ ps \in \mathbf{PS}, \tag{62}$$

$$\sum_{ps \in \mathbf{PS}} n^{h}_{p,o,tr,ps} \leq 1 \quad \forall\ p \in \mathbf{P}, o \in \mathbf{OL}_p,\ tr \in \mathbf{TR},\ ps \in \mathbf{PS}, \tag{63}$$

where $n^{h}_{p,o,tr,ps}$ is a binary variable which takes the value of 1 if the heat flow is in the corresponding standard piping size and 0 otherwise and $\dot{I}^{p}_{p,o,tr,ps}$ is the slack variable which takes the value of $\dot{Q}^{max}_{p,o,tr}$ if $n^{h}_{p,o,tr,ps}$ is 1 and 0 otherwise. The sizes of the resource pipes are determined similar to the heat pipes according to Equations (64)–(66).

$$\dot{m}^{lb}_{l,u,o,ps} \cdot n^{r}_{l,u,o,ps} \leq \dot{J}_{l,u,o,ps} \leq \dot{m}^{ub}_{l,u,o,ps} \cdot n^{r}_{l,u,o,ps} \quad \forall\ l \in \mathbf{L},\ u \in \mathbf{U}_l,\ o \in \mathbf{OL}_u,\ ps \in \mathbf{PS}, \tag{64}$$

$$\sum_{ps \in \mathbf{PS}} \dot{J}_{l,u,o,ps} = \dot{M}^{max}_{l,u,o,ps} \quad \forall\ l \in \mathbf{L},\ u \in \mathbf{U}_l,\ o \in \mathbf{OL}_u, \tag{65}$$

$$\sum_{ps \in \mathbf{PS}} n^{r}_{l,u,o,ps} \leq 1 \quad \forall\ l \in \mathbf{L},\ u \in \mathbf{U}_l,\ o \in \mathbf{OL}_u, \tag{66}$$

where $n^{r}_{l,u,o,ps}$ is a binary variable which takes the value of 1 if the resource flow uses the corresponding pipe size and 0 otherwise and $\dot{J}_{l,u,o,ps}$ is the slack variable which takes the value of $\dot{M}^{max}_{l,u,o,ps}$ if $n^{r}_{l,u,o,ps}$ is 1 and 0 otherwise.

After determining the piping sizes, their corresponding costs are calculated according to Equations (67) and (68), respectively. The total piping cost is then calculated by summing the heat and resource piping costs as presented in Equation (69).

$$C^{pipe_h}_{p,o,tr} = \sum_{ps \in \mathbf{PS}} \mathrm{c}^{\mathrm{pipe}}_{ps} \cdot \mathrm{tf} \cdot \mathrm{l}^{\mathrm{pipe}}_{lc,o} \cdot n^{h}_{p,o,tr,ps} \quad \forall\ p \in \mathbf{P},\ lc \in \mathbf{LC},\ o \in \mathbf{OL}_{lc},\ tr \in \mathbf{TR}, \tag{67}$$

$$C_{l,u,o}^{pipe_r} = \sum_{ps \in \mathbf{PS}} \mathrm{c}_{ps}^{\mathrm{pipe}} \cdot \mathrm{tf} \cdot \mathrm{l}_{lc,o}^{\mathrm{pipe}} \cdot n_{l,u,o,ps}^{r} \quad \forall\, l \in \mathbf{L},\ u \in \mathbf{U}_l,\ lc \in \mathbf{LC},\ o \in \mathbf{OL}_{lc}, \tag{68}$$

$$C^{\,pipe} = \left(\sum_{p \in \mathbf{P}} \sum_{o \in \mathbf{OL}_p} \sum_{tr \in \mathbf{TR}} C_{p,o,tr}^{pipe_h} + \sum_{l \in \mathbf{L}} \sum_{u \in \mathbf{U}} \sum_{o \in \mathbf{OL}_u} C_{l,u,o}^{pipe_r} \right) \cdot \mathrm{F}^{\mathrm{an}} \quad \forall\, l \in \mathbf{L},\ u \in \mathbf{U}_l,\ lc \in \mathbf{LC},\ o \in \mathbf{OL}_{lc}, \tag{69}$$

where tf is the trenching cost factor (TCF) which is 1 for above-ground pipes (i.e., no trenching) and 1.3 for underground pipes [55], $\mathrm{c}_{ps}^{\mathrm{pipe}}$ is the specific piping cost of the corresponding pipe size and $C^{\,pipe}$ is the total annualised piping cost for heat and resource exchange between the locations.

4. Case Study

The case study consists of eight locations, each containing a plant and its associated utilities. The locations are assigned with x and y coordinates to indicate their geographical position. It is assumed that all locations have the same altitude; hence, the distance between locations is calculated according to the Manhattan distance (MD). The locations and their plants are given as follows:

- Site 1: Low-temperature chemicals production plant. The process requires heat for pre-heating the reactants and re-boiling the bottoms streams of distillation columns. The products separated at the distillation columns are cooled by air in overhead coolers first and then by water in shell and tube heat exchangers. Electricity requirement in the site is due to mechanical drives such as pumps and compressors. The site energy profile is adapted from [56];
- Site 2: Medium-temperature chemicals production plant. Similar to the plant at Site 1, this process requires heating by steam and cooling by water and air as well as electricity for the mechanical drives. The only difference is that this site has a higher pinch point and production rate. The site energy profile is adapted from [56];
- Site 3: Brewery plant. Brewery consists of two main processes; beer production and bottling. In beer production the raw materials are mixed, boiled, fermented and pasteurised. Bottling includes several stages of cleaning. The heating requirement is mainly in the brewhouse for heating and boiling the mixture prior to fermentation [57] and electricity demand is mainly due to refrigeration systems. The model of the site is adapted from [58];
- Site 4: Cement plant with dry process. The Cement process is centered around clinker production which requires heat at high temperatures up to (1450 °C) for preheating the raw materials to temperature required for calcination. After the reaction, the product at high temperature is cooled and milled to give its final form. The heating requirement is satisfied by burning coal and alternative fuels in the kiln while cooling is done by air. Electricity is required to drive the mills and other mechanical equipment. The process is modelled according to [59];
- Site 5: Dairy plant. Dairy plants include processes for multiple products. Depending on the product slate, the process characteristics differ significantly. For example, condensed milk production is heating intensive while ice cream production mostly requires refrigeration. The plant in the case study is assumed to produce condensed milk and yogurt. The model is adapted from [59];
- Site 6: Pulp and paper production plant. Pulp and paper plants may utilise different technologies for pulp production whereas paper production is relatively standard. The main energy consumption of the plant is heat for drying paper and pulp. The model of the plant is adapted from [60];
- Site 7: Oil refinery. Refineries rely on distillation to separate different components of crude oil, followed by several chemical reactions to break large hydrocarbon molecules into smaller ones. The core of the plant, as well as the main energy consumer, is the crude oil distillation unit. Similar to the chemical plants, heat is required for the bottom streams of the distillation columns and reactions, while cooling is required to condense the overhead streams of the distillation columns. The refinery model is adapted from [59];
- Site 8: Waste incineration plant. Waste incineration plants are typically located near cities to provide heat to the district heating networks while producing electricity in the steam network. The plant is modelled according to [7].

As the focus of the method is energy consumption, only the flows related to energy (e.g., fuels, heat, electricity) are taken into account. Thus the raw material and intermediate flows within each plant are neglected. The product flowrates are indicated to provide a reference size of the plants. The locations of the plants can be seen in Figure 3.

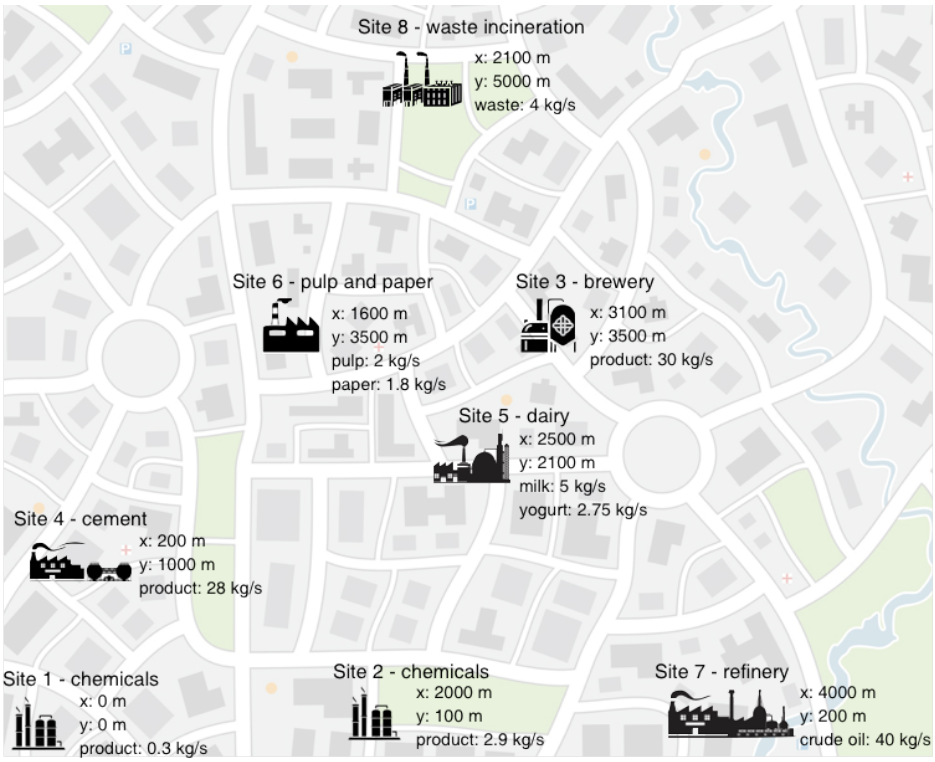

Figure 3. Case study layout.

The grand composite curves (GCCs) of the plants in Figure 4 give detailed information about the minimum heating and cooling requirements. The data used to construct the curves are given in the Appendix A.

4.1. Utility Systems and Resources

4.1.1. Existing Technologies on the Plants

Each plant in the system is considered to operate independently under current conditions. Thus, the sites have their own utility systems to close the energy balance and market access to close the resource balance. The utility systems that already exist on the sites are:

- Boiler: represents a combustion chamber which intakes natural gas and air and outputs heat. The boiler modelling is done according to [61] which assumes that the heat from natural gas consumption is delivered to the steam network by radiation and convection. Table 2 depicts the specifications of the boiler model;

Table 2. Boiler model specifications.

Stream	T^{in} [°C]	T^{out} [°C]	$\dot{q}$ [kW]
Fuel	-	-	1031
Radiation	827	827	656
Convection	827	100	324
Air preheating	25	150	−49

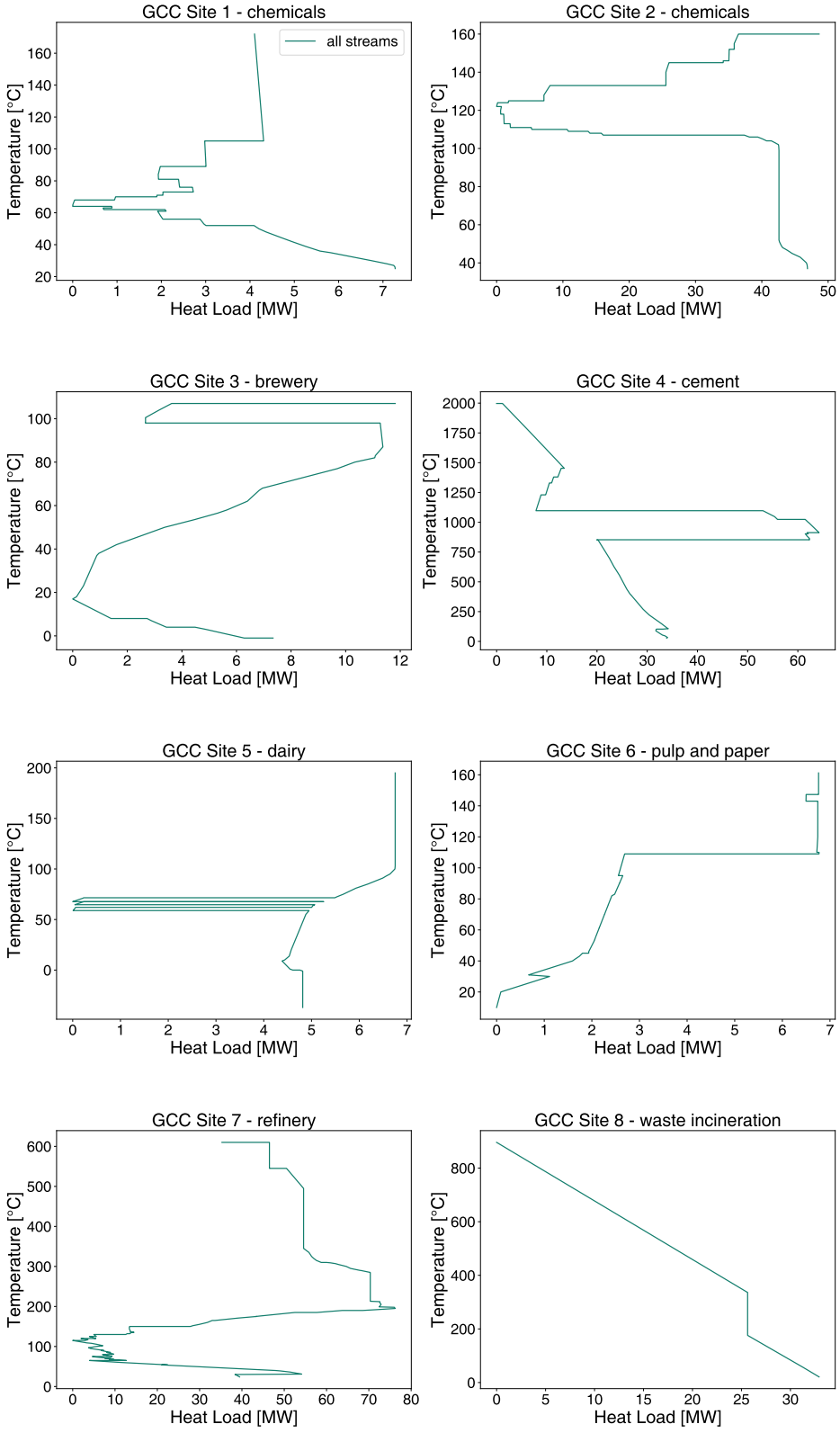

Figure 4. Grand composite curves (GCCs) of the processes in the case study.

- Steam network: an intermediate step between the boiler and processes. Heat is delivered to the steam network resulting in steam production. Afterwards, high pressure steam is turbined to cogenerate electricity and low pressure steam which is fed into the processes for heating.

The steam network model is adapted from [62]. Table 3 illustrates the configuration of the steam network in all locations except for Site 8. The configuration of the waste incineration steam network is adapted from [7];

Table 3. Configuration of the steam network.

Type	Header Pressure [bara]	Header Temperature [°C]	Turbine
Production/Distribution	45	367	yes
Distribution	24	228	yes
Distribution	8	175	yes
Distribution	4	150	no
Production/Distribution	2	126	no
Production/Distribution	1	105	no

- Cooling systems: consist of cooling towers and aerocoolers. Cooling water is used to remove heat from the processes which is then discharged to the environment at the cooling tower. The cooling tower model (see Table 4) is adapted from [63]. Aerocooling is modelled as a simple fan according to [56].

Table 4. Water cooling specifications.

Stream	T^{in} [°C]	T^{out} [°C]	$\dot{q}$ [kW]	$\dot{m}$ [kg/s]	$\dot{e}$ [kW]
Supply	15	25	−1000	-	-
Return	25	15	1000	-	-
Make-up water	-	-	-	0.34	-
Electricity	-	-	-	-	10

- Refrigeration: is needed for the processes requiring sub-atmospheric temperatures (e.g., brewery, dairy). A simple refrigeration cycle model (see Table 5) is used which provides the process-specific refrigeration temperature and assuming a coefficient of performance of 3 [7].

Table 5. Refrigeration cycle specifications.

Stream	T^{in} [°C]	T^{out} [°C]	$\dot{q}$ [kW]	$\dot{e}$ [kW]
Evaporation	−5	−5	−1000	-
Condensation	35	35	1333	-
Electricity	-	-	-	333

4.1.2. Additional Technologies for Improvements

In addition to the existing utility systems, new energy conversion technologies can be purchased and installed to improve the overall energy efficiency and operating cost. The additional utilities considered in the case study are:

- HPs: are ideal in the cases where the pinch temperature is low and heat transfer from below to above the pinch point with low temperature lift is possible. Considering the GCCs presented in Figure 4, Site 1, Site 2, Site 5 and Site 7 offer potentials for heat pump integration. The evaporation and condensation temperatures of the HPs are selected manually based on the GCCs. Table 6 depicts the specifications of the HPs;

Table 6. Heat pump specifications.

	T^{evap} [°C]	T^{cond} [°C]	$\dot{q}^{evap}$ [kW]	$\dot{q}^{cond}$ [kW]	$\dot{e}^{comp}$ [kW]
HP_{site1}	58	73	−1008	1067	59
HP_{site2}	100	130	−716	797	81
HP_{site5}	82	107	−1035	1131	96
HP_{site7}	100	130	−716	797	81

- Mechanical vapour recompressions (MVRs): similar to HP but instead of using an intermediate fluid, the vapour is directly compressed to a higher pressure and temperature. Potential MVR integration at Site 3 and Site 6 is considered. Steam can be imported at 1 bar from the other locations and compressed to 2 bar instead of producing it in the boilers.
- Cogeneration Engines: commonly used in industrial sites as they provide both heat and electricity. Similar to HP, pinch point plays an important role in the integration of cogeneration engines. A significant part of the heat comes from the cooling water of the engine. Thus, they are suitable only for the processes with low pinch temperatures such as Site 1, Site 3, Site 5 and Site 6. The specifications of the cogeneration engines (see Table 7) are adapted from [56].

Table 7. Cogeneration engine specifications.

Stream	T^{in} [°C]	T^{out} [°C]	$\dot{q}$ [kW]	$\dot{e}$ [kW]
Fuel	-	-	2605	-
Exhaust Gasses	470	120	537	-
Engine Cooling	87	80	653	-
Electricity	-	-	-	1063

- Photo-voltaics (PVs): have the potential to supply the electricity requirement of the industrial processes as well as the utility systems (e.g., HPs). The limitations for PV integration are availability of land and high capital investment. As the industrial plants are generally located outside urban centres, it is assumed that there is enough land and roof surface to install them. The PV model (see Table 8) is adapted from [7] for a reference area of 100 m^2.

Table 8. Photo-voltaic (PV) specifications.

	T^{in} [°C]	T^{out} [°C]	$\dot{q}$ [kW]	$\dot{e}$ [kW]
PV	-	-	-	16.6

4.1.3. Utility and Resource Costs

Energy conversion technologies not initially available on the sites require investment for the purchase and installation of the equipment. The HPs consist of two heat exchangers (i.e., evaporator and condenser) and a compressor while the MVRs require investment only in a compressor. The cost of the heat exchangers and compressors is calculated according to [64]. The non-linear cost functions are linearised within the range of application [f_u^{min}, f_u^{max}] to be coherent with the MILP framework. The fixed and variable investment cost (c_u^{inv1} and c_u^{inv2}, respectively) of the additional technologies are listed in Table 9 and affect the objective function by inclusion in Equation (4).

The operating cost of the system is calculated based on the resource and energy consumption. Since raw materials and intermediate products are excluded from the analysis, only the costs of electricity, water and fuels are considered. Table 10 illustrates the specific cost of the main contributors to the operating cost. The specific cost [65], share in the fuel mix [66] and properties [67] of the alternative fuels used in the cement plant are given in the Appendix A.

Table 9. Costing and sizing parameters of the additional energy conversion technologies.

Unit	c^{inv1} [€/year]	c^{B} [€/year]	f^{min} [-]	f^{max} [-]
HP_{site1}	8774	54,521	0.1	5
HP_{site2}	5270	22,328	0.1	30
HP_{site5}	8425	46,909	0.1	10
HP_{site7}	5270	22,328	0.1	10
MVR_{site3}	2265	26,950	0.1	4
MVR_{site6}	4595	38,142	0.1	2
Co-gen_{site1}	11,910	119,095	0.1	1
Co-gen_{site3}	11,910	119,095	0.1	1
Co-gen_{site5}	11,910	119,095	0.1	1
Co-gen_{site6}	11,910	119,095	0.1	1
PV	0	70,730	0	100

Table 10. Specific cost of the main fuels and resources.

Unit	c^{spec}
Natural gas	0.030 [€/kWh]
Coal	0.600 [€/kg]
Electricity purchase	0.092 [€/kWh]
Electricity selling	0.055 [€/kWh]
Water	0.070 [€/t]

5. Results and Discussion

The method is first applied to two of the plants presented in the case study introduced in Section 4 to analyse the results in deeper detail. The optimisation of the overall case study is also completed to display the capability and effectiveness of the method in solving large-scale, complex industrial problems.

5.1. Symbiosis between Two Chemical Plants

The two chemical plants introduced in the case study represent an opportunity for industrial symbiosis by heat sharing. Site 2 has a higher pinch point than Site 1, thus its excess heat can be recovered and used in Site 1. Figure 5 illustrates the results of parametric optimisation in which the sum of the operating and utility investment cost of the plants is minimised while the investment in piping between the plants is constrained with a limit (ϵ). Figure 5a exhibits the trade-off between the two objectives while the colour indicates the sum of both (i.e., total cost with piping). The minimum total cost with piping is obtained in Solution 6 when a cogeneration engine is installed on Site 1 and a heat pump on Site 2 while heat is shared between the sites with 1 bar steam; however, similar total cost results are obtained with other solutions where investments in piping are between 0 and 0.3 M€. As the investment cost limit for the pipeline between plants is increased, lower piping-exclusive total cost is obtained. This decrease coincides with lower operating cost due to excess heat recovery between the sites. Investment decisions also vary with respect to the limit on the piping investment. For example, investment on Site 1 HP decreases in correlation with piping investments because the imported steam from Site 2 replaces the HP. Conversely, integration of the cogeneration engine on Site 1 is independent of the piping allowance as the decision of installing the cogeneration engine is driven by the electricity generation rather than heat. PV is not integrated in any of the solutions as its capital investment cost is higher than the associated operating cost benefits. Figure 5b reveals further details about the solutions of parametric optimisation focusing on total investment cost including piping and heat sharing between the sites. When investment on piping between the sites is not allowed (Solution 1, piping cost = 0 M€/year), the optimal solution is investing in HPs on both sites and a cogeneration engine on Site 1. As the limit on piping investment increases, 1 bar steam exchange becomes part of the optimal solution. When 1 bar steam import reaches its limit (solution 6, piping cost = 0.29 M€/year),

the investments in exchanging 2 bar steam are made. When heat sharing and losses are considered, a significant decrease in the heat losses in the last solution (solution 10, piping cost = 0.53 M€/year) is observed, although the absolute heat exchanged remains the same as underground pipes are selected given the high allowance on piping cost. The same phenomenon can be observed comparing solutions 8 (piping cost = 0.41 M€/year) and 9 (piping cost = 0.45 M€/year). In the latter solution, more 2 bar steam is shared but heat losses are lower due to installation of underground pipes.

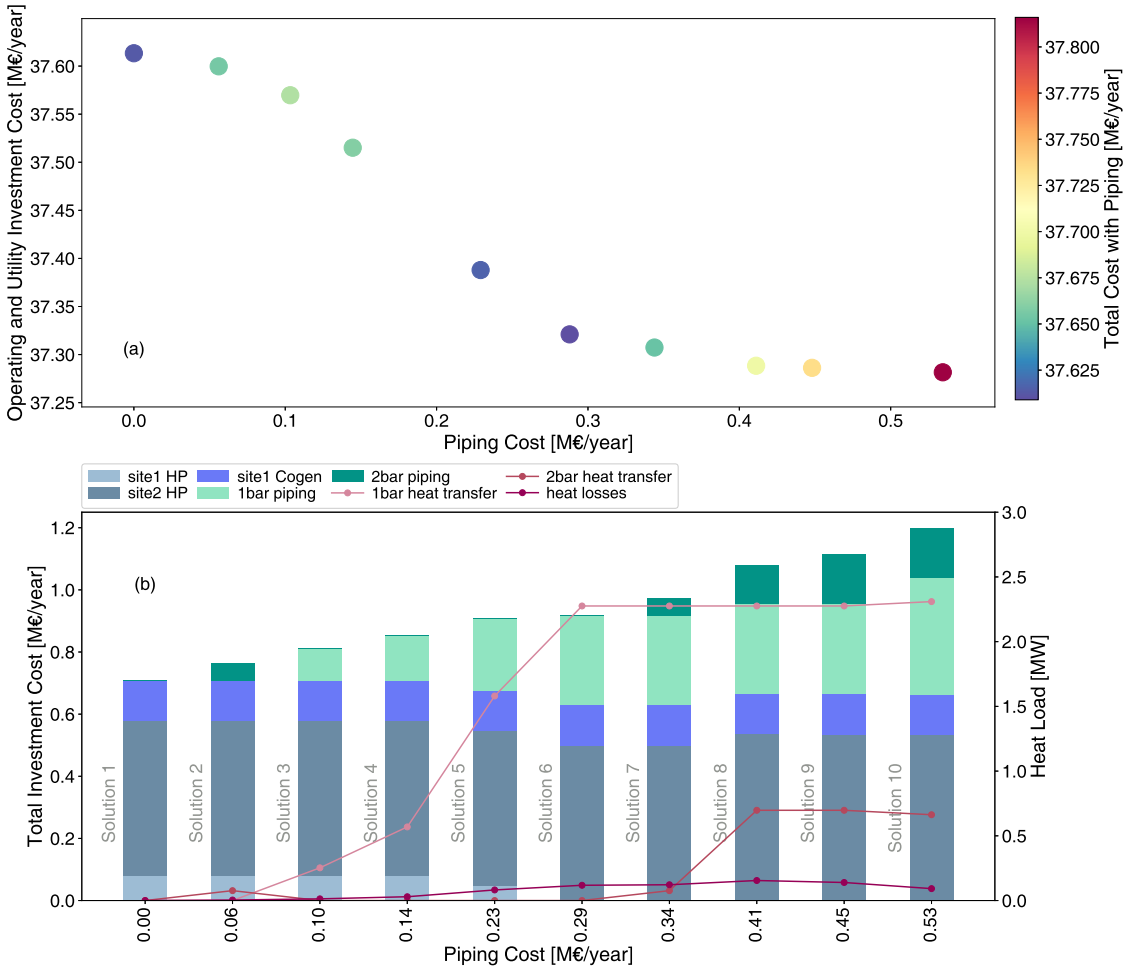

Figure 5. Parametric optimisation with two chemical plants. (**a**) pareto frontier; (**b**) investment cost breakdown and heat sharing.

Figure 6 depicts the Carnot composite curves (CCCs) of Site 1 and Site 2 which provide more detail about heat integration. HP at Site 1 is partially replaced by 1 bar steam import when solutions 1 and 4 are compared. In solution 7, 1 bar steam import from Site 2 completely replaces the HP at Site 1. Moreover, the size of the HP at Site 2 increases to produce 2 bar steam and export it to Site 1. In solution 10, the boiler at Site 1 is completely substituted by 1 and 2 bar steam imports.

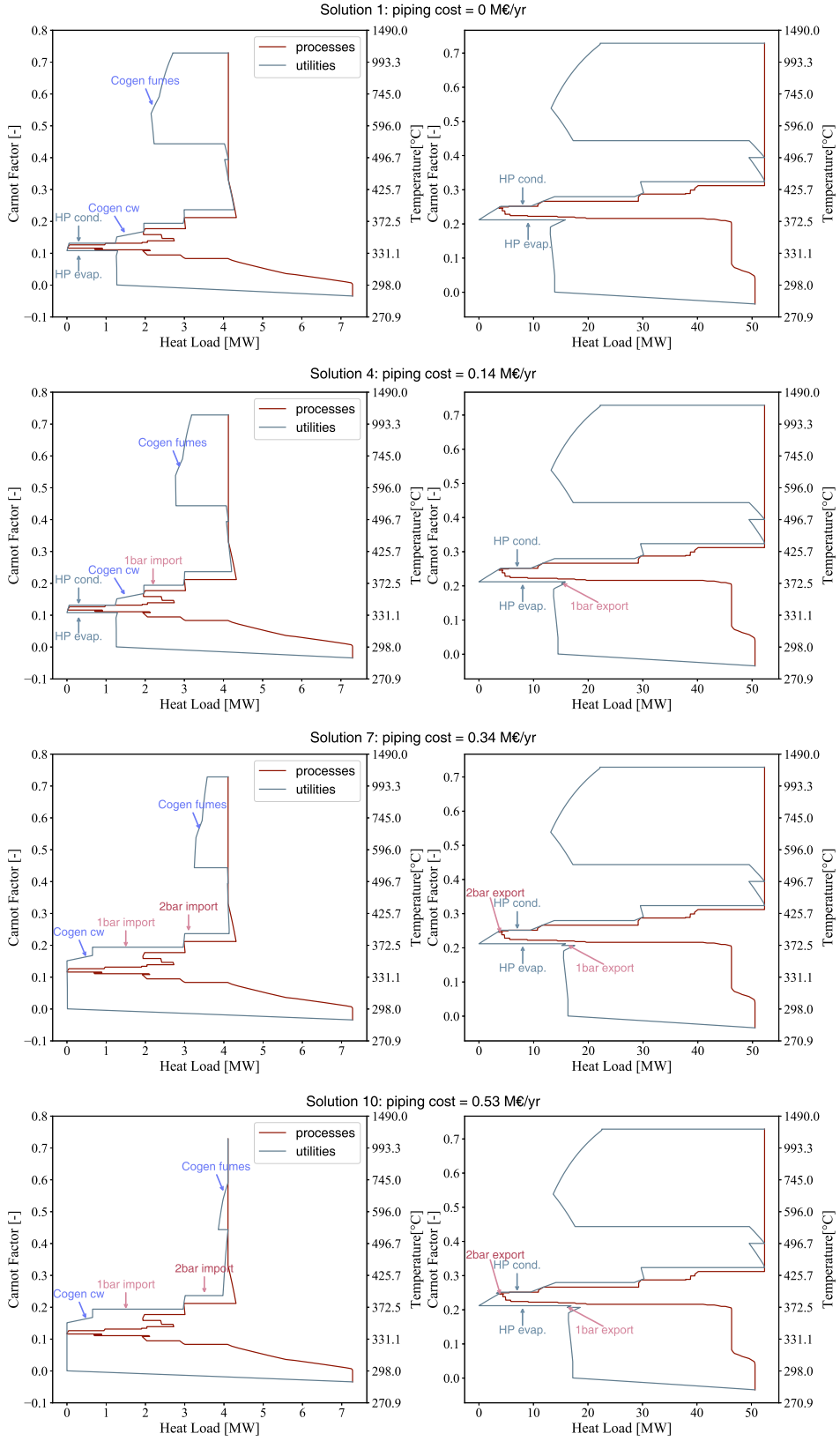

Figure 6. CCCs of Site 1 (**left**) and Site 2 (**right**) with different piping cost investment limits.

5.2. Symbiosis between All Plants

Optimisation of the case study introduced in Section 4 with all plants was completed to exhibit the capability of the method to solve complex, large-scale problems. Sites 2 and 7 have excess heat, while Sites 1, 3, 5 and 6 require heating at relatively low temperatures. In addition, the waste incineration plant at Site 8 can provide steam to the other locations instead of turbining and condensing it at low pressure. Thus, there is a large potential for heat sharing between the locations. The transfer of heat can be done only via utility systems. As there is a steam network in each location except Site 4, steam is considered to be the transfer fluid. In addition to symbiosis by sharing heat, there is a possibility to share material from Site 1 to Site 4, as the cement process can use chemical waste as a fuel. Similar to the case with two chemical plants, the total cost of the system excluding the piping cost is minimised, while constraining the piping investment cost at different limits.

Figure 7a depicts the parametric optimisation results. Similar to Section 5.1, the operating and utility investment cost decreases as the limit on piping investment is increased. Considering all cost elements, the minimum is obtained when the piping cost is ∼2.2 M€/year. Other solutions show that the operating and utility cost can be further decreased; however, the additional piping cost is larger than the associated economic benefit. A further ∼6 M€/year investment in piping to connect the sites only results in marginal improvement in the main objective. The breakdown of total investment cost can be seen in Figure 7b, as well as the amount of heat sharing and losses. In solutions with a low piping cost limit (similar in magnitude to the utility investment cost), all investments are relatively small. With increasing limits on the piping investment, it quickly dominates the investment cost distribution as heat sharing can be done over long distances and with high flowrates. At low piping investment limits, the investment goes toward sharing high pressure steam since it requires smaller pipe diameter. As the limit on the piping cost increases, heat sharing switches to lower pressure (i.e., lower temperature) steam as lower temperature corresponds to lower heat losses. With increasing allowance, heat losses trend upward until the pipe investment cost reaches ∼6.6 M€/year as more heat is shared between the sites. Past this level, despite stable or increased heat sharing, heat losses start decreasing since higher allowance on piping cost permits investment in underground pipes which are naturally more insulated.

Figure 8 illustrates the layout of the plants and their connections for four solutions with different piping investment levels from parametric optimisation (highlighted in Figure 7b. The switch from high to low pressure steam sharing can be observed by comparing solutions with lower (e.g., Figure 8a) and higher piping investments (e.g., Figure 8b). Sharing chemical waste with the cement plant is activated with a low piping investment allowance. Heat sharing is selected using above-ground pipes at low piping investment solutions (e.g., Figure 8a), while increasing this allowance first encourages a mixture of above-ground and underground pipes (e.g., Figure 8b,c) and then only underground pipes (e.g., Figure 8d). With large piping investment limits, even very small heat sharing options (<1 MW) are activated, which might not be practically feasible.

5.3. Piping Investment by a Third Party

Although investment in inter-plant infrastructure has proven economic benefits, industries are often reluctant to partake in such projects as they include several companies and the payback time may not fit within stringent economic policies. In such cases, the involvement of a third party could be considered. The analysis presented in Section 5.2 examines the piping investment to be made by industries but the same investment could alternatively be made by a third party with less stringent payback requirements. The investment to be made by such a third party would be recuperated by providing steam at a slight premium compared to the cost of generation. Such a strategy mitigates industrial risk and investment while providing improvements in operating cost and business opportunities for utility providers, which use different business models than the large process industries. The steam price provided to the industries is calculated to recuperate the piping cost over the time horizon of the installation and an additional premium to realise profitability for

the third party. The steam premium is varied between 0%—representing a non-profit third party or shared industrial investment—to 20%, providing a business case for the third party to compensate the investment and be profitable. The results are compared in Figure 9a based on the overall system profit. The baseline for the profitability analysis is the solution in which piping cost is zero, that is, there is no sharing between the industries and each plant pays for its own energy technologies. For the other solutions, the system profit is calculated as the difference between the change in operating cost and the annualised investment cost including piping. As the steam price premium increases, the profitable zone narrows and the highest potential profit decreases, since a higher price is paid for the same operating cost savings, due to the profit margin of the third party. The solutions with different steam price premiums selected in Figure 9a are compared in terms of steam price in Figure 9b. The price of steam is calculated as the ratio between the cost of piping including the profit margin of the third party and the total amount of steam shared between sites. The savings on steam price for the industries (compared to the break-even price) range between 47% and 32%. With increasing third-party profit, the steam price increases; however, it remains well below the break-even price.

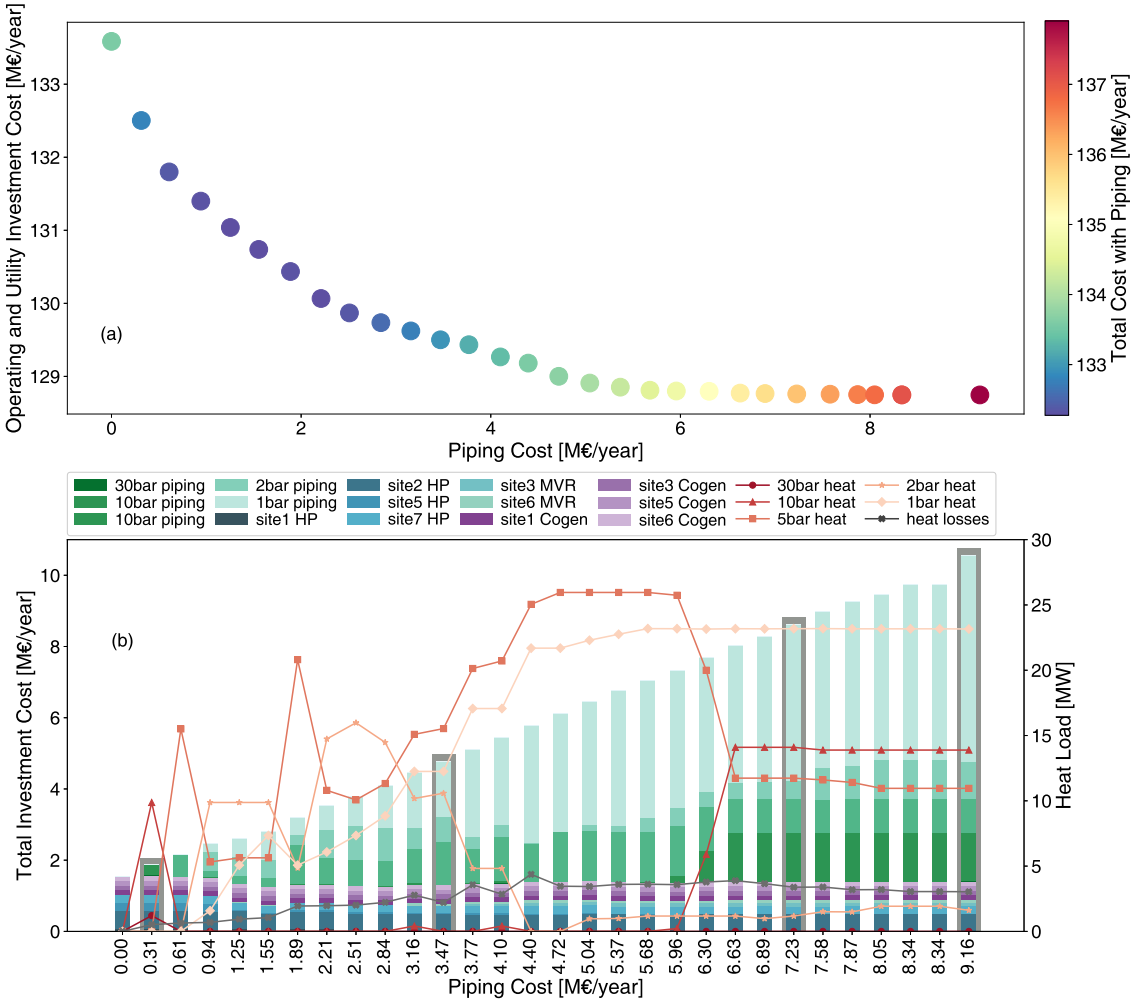

Figure 7. Parametric optimisation results for an industrial complex (**a**) pareto frontier; (**b**) investment cost breakdown and heat sharing.

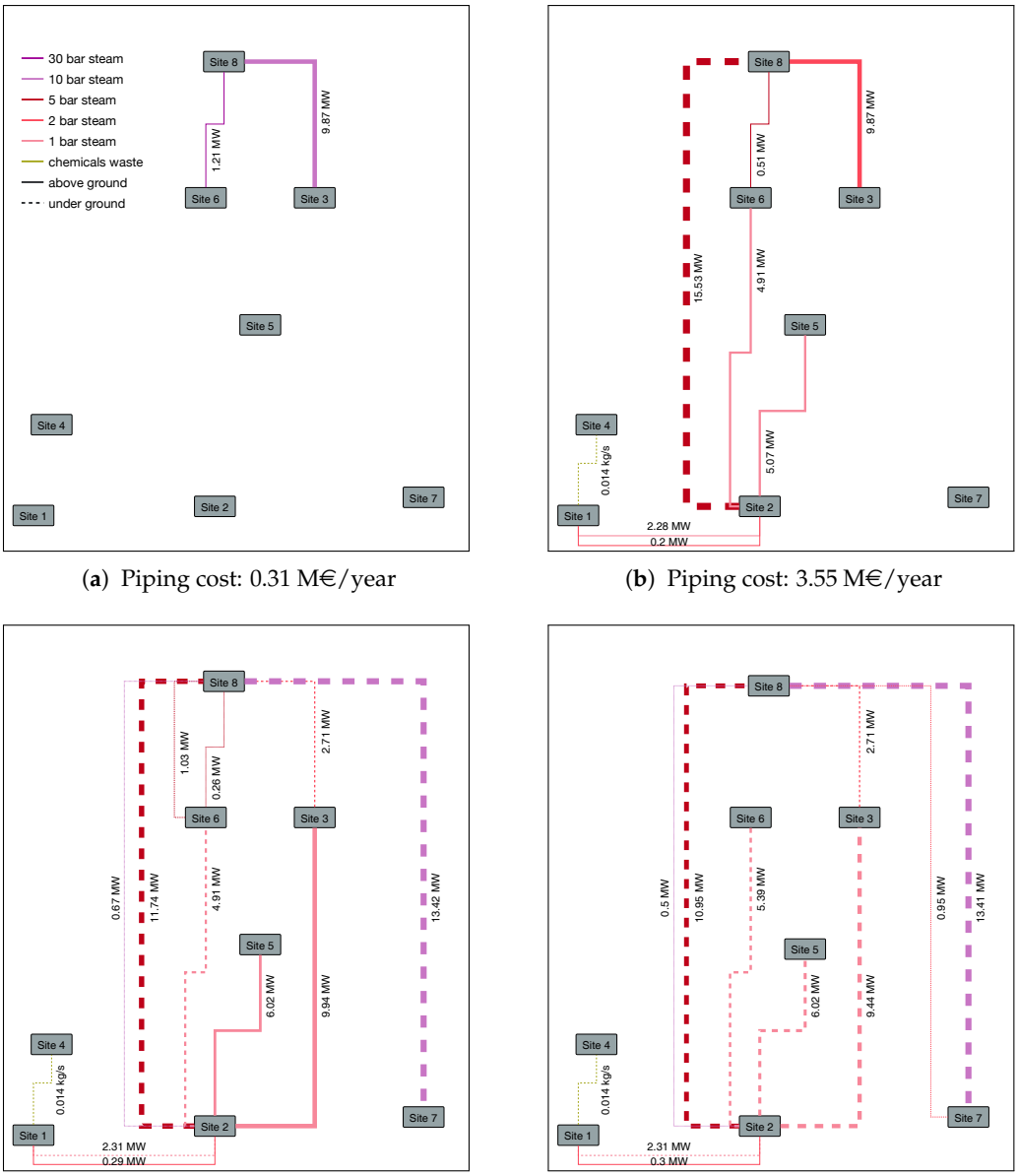

(**a**) Piping cost: 0.31 M€/year

(**b**) Piping cost: 3.55 M€/year

(**c**) Piping cost: 7.48 M€/year

(**d**) Piping cost: 9.42 M€/year

Figure 8. Optimal piping connections at different investment levels.

5.4. Comparison with Baseline and State of the Art

The baseline operation of the sites represent their current state in which little or no heat is recovered, better performing technologies (e.g., HPs) are not integrated and heat and resources are not shared between locations. The baseline fuel and electricity consumption of the sites is modelled according to [56,59]. State-of-the-art methods do not consider the location aspects, as discussed in Section 2; thus, processes in different locations can exchange heat and resources without any restriction. Table 11 compares economic and environmental key performance indicators (KPIs) of the overall system in the baseline state, when a state-of-the-art targeting method [44] is used and when the proposed method is used. The objective function is modified in this case to include the piping cost. Compared to the baseline, the total cost and CO_2 emissions of the system decrease by 21% and 35%, respectively, using the proposed method. This is partially due to the integration of new energy conversion technologies and partially because of heat and resource sharing between the locations as discussed in the previous sections. The reduction in the economic objective function and CO_2 emissions

reach 33% and 48%, respectively, using the targeting approach. Although the targeting method offers further reduction in the cost, it represents only the theoretical potential while the proposed method takes the practical constraints of locations and piping investment into account.

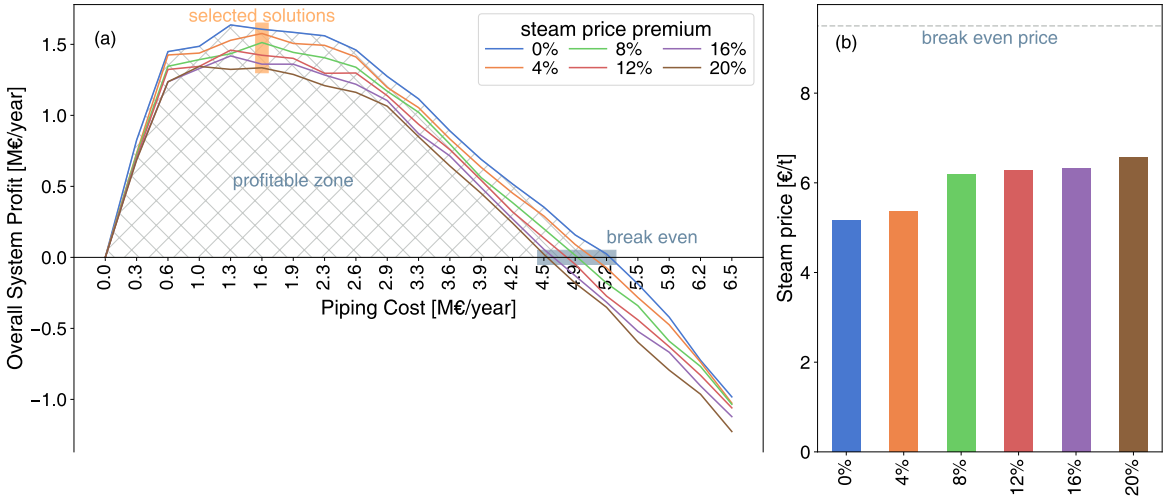

Figure 9. Overall profitability (**a**) and steam price (**b**) considering the premium charged by a third party.

Table 11. Comparison of the results of the present work with the baseline and targeting approach.

KPI	Unit	Baseline	State of the Art	This Work
Operating cost	M€/year	167.8	111.4	128.8
Utility investment cost	M€/year	0	1.1	1.3
Piping cost	M€/year	0	0	2.2
Total	M€/year	167.8	112.6	132.2
CO_2 emissions	Mt/year	867	452	562

6. Conclusions

This work proposes a PI method considering location aspects. Consequently, the heat cascade is reformulated to account for heat distribution losses and temperature drops, while the electricity balance is modified to include pumping work required to compensate pressure drops. The cost of the infrastructure between the plants is also considered in the form of piping cost and the resulting problem is formulated using MILP. Parametric optimisation is employed to systematically generate multiple solutions.

The method is first applied on a scenario with two chemical plants, to study the potential heat sharing between them. The results show that the lowest total cost solution is achieved by sharing 1 bar steam between the plants, with a cogeneration engine installed in one plant and a HP is integrated in each. Other solutions are also found, which prove the possibility of eliminating the main heating utility of one plant by multi-level steam sharing.

As a large-scale application of the method, parametric optimisation on eight industrial plants in geographical proximity is also completed. In this case, with small piping investment budgets, the optimal solutions favour sharing heat via high-pressure steam, since higher pressure levels require smaller pipe diameters. With larger budgets, lower pressure steam sharing options emerge, stemming from reduced heat losses. Following the same trend, above-ground pipes are preferred at low piping cost limits, while underground pipes are selected at high limits, due to the trade-off between heat losses and piping investment.

When process industries are not willing to take the risk of investing in inter-plant infrastructure, involvement of a third party can be beneficial. The third-party, making the initial investment and selling steam between plants, could be a non-profit governmental organisation or a utility company

with profitability targets. In either case, solutions resulting in overall system profit are obtained, with lower system profit at higher steam price premiums. Industries benefit from such a strategy by avoiding investment risks while benefitting from a 40% reduction in steam prices (on average) with the third party profiting from a steam price premium of up to 20%.

The optimal results obtained using the proposed method lead to a 21% and 35% reduction in the total cost and CO_2 emissions, respectively, compared to the baseline operation of the sites, resulting from heat and resource sharing between the sites and integrating new energy conversion systems. The theoretical optimum suggested by the targeting approach results in an even lower total cost and environmental impact; however, contrary to the work presented in this paper, it does not account for technical constraints (e.g., using commercially available technologies) or economic constraints (e.g., including the investment cost of the new technologies or the piping cost).

The present work provides a complete analysis for industrial symbiosis with heat and resource sharing as well as a set of options for investment budgets on inter-plant infrastructure. Heat losses and pumping work requirements are assumed to scale linearly with the flow for inclusion within the MILP framework. Such assumptions simplify the model solution process but may result in missing the global optimum solution. Thus, further analysis should be carried out, studying non-linearity aspects and their impact in the results. Moreover, large industrial retrofit projects, as the one presented in this work, are generally carried out over a long time horizon. Hence, future work should include investment scheduling analysis of the system, which will offer insight into the timeline of the investment in new technologies and piping as well as utility replacement requirements.

Author Contributions: Conceptualization, H.B., I.K. and F.M.; methodology, H.B.; software, H.B.; validation, H.B. and I.K.; formal analysis, H.B. and I.K.; investigation, H.B., I.K. and F.M.; resources, F.M.; data curation, H.B.; writing–original draft preparation, H.B.; writing–review and editing, H.B. and I.K.; visualization, H.B.; supervision, I.K. and F.M.; project administration, I.K. and F.M.; funding acquisition, F.M.

Funding: This research project is financially supported by the Swiss Innovation Agency lnnosuisse and is part of the Swiss Competence Center for Energy Research SCCER EIP. This project has received funding from the European Union's Horizon 2020 research and innovation programme under grant agreement No 679386. This work was supported by the Swiss State Secretariat for Education, Research and Innovation (SERI) under contract number 15.0217.

Conflicts of Interest: The authors declare no conflict of interest.

Appendix A

Appendix A.1 Heat Stream Data of the Processes

The heat streams of the plants in the case study are listed in Tables A1–A7 respectively. The stream information includes inlet and outlet temperatures and inlet and outlet enthalpies.

Table A1. Site 1 heat streams.

Stream	T^{in} [°C]	T^{out} [°C]	H^{in} [kW]	H^{out} [kW]
s1p1	51	56	0	10
s1p2	56	56	0	192
s2p1	79	84	0	54
s2p2	84	84	0	1032
s3p1	61	66	0	7
s3p2	66	66	0	135
s4p1	58	63	0	47
s4p2	63	63	0	900
s5p1	60	65	0	49
s5p2	65	65	0	931
s6p1	43	100	0	49

Table A1. *Cont.*

Stream	T^{in} [°C]	T^{out} [°C]	H^{in} [kW]	H^{out} [kW]
s6p2	100	100	0	938
s7p1	43	100	0	21
s7p2	100	100	0	391
s8p1	63	68	0	36
s8p2	68	68	0	685
s9p1	53	58	0	11
s9p2	58	58	0	200
s10	53	31	305	0
s11	50	38	23	0
s12	41	32	1109	0
s13	55	33	575	0
s14	44	31	123	0
s15	47	30	72	0
s16p1	67	67	538	0
s16p2	67	40	132	0
s17p1	86	86	452	0
s17p2	86	40	134	0
s18p1	57	57	1084	0
s18p2	57	35	160	0
s19p1	67	67	526	0
s19p2	67	40	117	0
s20p1	67	67	319	0
s20p2	67	40	71	0
s21p1	69	69	881	0
s21p2	69	40	247	0
s22p1	177	61	354	0
s22p2	61	61	840	0
s22p3	61	40	93	0
s23p1	81	81	290	0
s23p2	81	40	75	0
s24	58	40	340	0

Table A2. Site 2 heat streams.

Stream	T^{in} [°C]	T^{out} [°C]	H^{in} [kW]	H^{out} [kW]
s1p1	135	140	0	95
s1p2	140	140	0	1805
s2p1	135	140	0	290
s2p2	140	140	0	5510
s3p1	150	155	0	640
s3p2	155	155	0	12160
s4p1	142	147	0	40
s4p2	147	147	0	760
s5p1	136	141	0	45
s5p2	141	141	0	855
s6p1	135	140	0	5
s6p2	140	140	0	95

Table A2. *Cont.*

Stream	T^{in} [°C]	T^{out} [°C]	H^{in} [kW]	H^{out} [kW]
s7p1	135	140	0	40
s7p2	140	140	0	760
s8p1	123	128	0	920
s8p2	128	128	0	17480
s9p1	114	119	0	85
s9p2	119	119	0	1615
s10p1	115	120	0	10
s10p2	120	120	0	190
s11p1	115	120	0	45
s11p2	120	120	0	855
s12p1	115	120	0	210
s12p2	120	120	0	3990
s13p1	115	120	0	15
s13p2	120	120	0	285
s28	49	44	200	0
s29	50	45	100	0
s30	51	46	100	0
s31	53	48	1100	0
s32	50	45	900	0
s33	53	48	500	0
s34	56	51	200	0
s35	52	47	100	0
s36	49	44	100	0
s37	57	52	400	0
s38	47	42	100	0
s39	56	51	100	0
s40	54	49	300	0
s41	48	43	100	0
s42p1	115	115	4950	0
s42p2	115	110	550	0
s43p1	112	112	19080	0
s43p2	112	107	2120	0
s44p1	115	115	360	0
s44p2	115	110	40	0
s45p1	111	111	1260	0
s45p2	111	106	140	0
s46p1	123	123	450	0
s46p2	123	118	50	0
s47p1	118	118	900	0
s47p2	118	113	100	0
s48p1	112	112	2205	0
s48p2	112	107	245	0
s49p1	113	113	1710	0
s49p2	113	108	190	0
s50p1	114	114	2970	0
s50p2	114	109	330	0
s51p1	116	116	3150	0

Table A2. *Cont.*

Stream	T^{in} [°C]	T^{out} [°C]	H^{in} [kW]	H^{out} [kW]
s51p2	116	111	350	0
s52p1	127	127	720	0
s52p2	127	122	80	0
s53p1	109	109	720	0
s53p2	109	104	80	0

Table A3. Site 3 heat streams.

Stream	T^{in} [°C]	T^{out} [°C]	H^{in} [kW]	H^{out} [kW]
s1	65	85	0	396
s2	85	60	742	0
s3	40	60	0	743
s4	40	20	1121	0
s5	15	85	0	63
s6	15	60	0	46
s7	15	85	0	2022
s8	35	60	0	627
s9	1	1	672	0
s10	6	1	1122	0
s11	1	15	0	1291
s12	70	5	7631	0
s13	15	80	0	7624
s14	48	65	0	296
s15	48	65	0	660
s16	15	52	0	581
s17	15	55	0	1294
s18	65	75	0	579
s19	105	100	27	0
s20	100	100	5478	0
s21	100	25	758	0
s22	15	80	0	5419
s23	78	105	0	2612
s24	105	105	0	5214
s25	5	80	0	1347
s26	103	10	8536	0
s27	10	10	840	0
s28	10	6	367	0
s29	6	6	668	0

Table A4. Site 4 heat streams.

Stream	T^{in} [°C]	T^{out} [°C]	H^{in} [kW]	H^{out} [kW]
s1	1450	650	37	0
s2	650	250	37	0
s3	250	100	37	0
s4	860	850	348	0
s5	890	880	668	0

Table A4. *Cont.*

Stream	T^{in} [°C]	T^{out} [°C]	H^{in} [kW]	H^{out} [kW]
s6	1531	1504	268	0
s7	860	700	1268	0
s8	1719	1531	328	0
s9	880	860	133	0
s10	560	390	1468	0
s11	104	50	2115	0
s12	250	100	37	0
s13	1822	1719	387	0
s14	1222	1177	89	0
s15	1177	1050	30	0
s16	390	104	1597	0
s17	104	45	9	0
s18	650	250	37	0
s19	700	560	1166	0
s20	1000	1000	37	0
s21	2000	2000	566	0
s22	1504	1222	357	0
s23	1450	650	37	0
s24	2000	1822	953	0
s25	25	104	0	113
s26	25	56	0	1255
s27	85	100	0	1255
s28	390	104	2652	0
s29	100	100	0	1255
s30	56	85	0	1255
s31	390	104	2477	0
s32	100	104	0	1255
s33	560	390	9018	0
s34	700	560	7807	0
s35	880	860	1200	0
s36	860	700	9297	0
s37	1177	1050	2710	0
s38	2000	1822	3124	0
s39	1719	1531	3882	0
s40	1504	1222	5864	0
s41	1531	1504	338	0
s42	1222	1177	895	0
s43	2000	2000	606	0
s44	1822	1719	1954	0
s45	25	40	0	62
s46	25	60	0	26
s47	626	850	0	11514
s48	850	850	0	39975
s49	850	860	0	348
s50	850	890	0	541
s51	1100	1100	45208	0
s52	1100	890	11358	0

Table A4. *Cont.*

Stream	T^{in} [°C]	T^{out} [°C]	H^{in} [kW]	H^{out} [kW]
s53	25	400	0	37
s54	25	1000	0	37
s55	25	225	0	37
s56	150	35	3613	0
s57	225	35	1598	0
s58	104	35	1300	0
s59	115	35	1287	0
s60	400	35	3126	0
s61	390	150	8202	0
s62	50	268	0	9018
s63	268	437	0	7807
s64	437	626	0	9297
s65	850	850	0	1200
s66	850	850	1	0
s67	910	910	0	2401
s68	910	1027	0	3609
s69	850	900	0	1651
s70	1377	1450	0	2281
s71	1027	910	146	0
s72	1227	1227	0	921
s73	910	900	25	0
s74	900	850	153	0
s75	1327	1377	0	1509
s76	900	910	0	324
s77	900	900	0	596
s78	1377	1377	0	843
s79	1227	1027	85	0
s80	850	850	0	1212
s81	1027	1027	5525	0
s82	1327	1327	0	445
s83	1450	1450	0	606
s84	1027	1227	0	5948
s85	1227	1327	0	2961

Table A5. Site 5 heat streams.

Stream	T^{in} [°C]	T^{out} [°C]	H^{in} [kW]	H^{out} [kW]
s1	66	98	0	12
s2	98	4	35	0
s3	86	4	277	0
s4	4	66	0	236
s5	66	86	0	68
s6	6	4	8	0
s7	69	69	0	−1051
s8	61	61	0	988
s9	66	15	94	0
s10	4	66	0	236

Table A5. *Cont.*

Stream	T^{in} [°C]	T^{out} [°C]	H^{in} [kW]	H^{out} [kW]
s11	70	70	0	1051
s12	66	66	0	−1005
s13	60	60	0	−988
s14	66	66	0	1005
s15	60	15	81	0
s16	69	15	102	0
s17	98	4	35	0
s18	20	10	73	0
s19	6	4	8	0
s20	4	20	0	118
s21	−21	−25	11	0
s22	7	−21	67	0
s23	−21	−21	0	−60
s24	4	95	0	342
s25	6	4	8	0
s26	83	3	254	0
s27	20	73	0	166
s28	−6	−6	1	0
s29	73	83	0	32
s30	3	−6	26	0
s31	−6	−6	0	−197
s32	−6	−35	80	0
s33	75	15	13	0
s34	5	5	30	0
s35	15	55	0	17
s36	67	80	0	21
s37	65	15	10	0
s38	59	70	0	19
s39	69	15	102	0
s40	4	90	0	327
s41	66	15	94	0
s42	100	170	0	447
s43	100	170	0	165
s44	170	170	0	3057
s45	35	35	0	122
s46	0	−3	205	0
s47	5	1	1105	0
s48	69	75	0	116
s49	105	105	0	472
s50	170	170	0	1132
s51	44	25	713	0
s52	9	26	0	300
s53	170	190	0	73
s54	78	78	0	179
s55	44	44	0	−2260
s56	35	35	0	551
s57	79	85	0	18

Table A5. *Cont.*

Stream	T^{in} [°C]	T^{out} [°C]	H^{in} [kW]	H^{out} [kW]
s58	6	28	0	1110
s59	95	95	0	179
s60	48	75	0	1238
s61	75	4	3257	0
s62	6	48	0	2046
s63	66	76	0	195
s64	85	85	0	857
s65	54	4	151	0
s66	44	5	118	0
s67	170	190	0	27
s68	70	70	0	225
s69	15	55	0	145
s70	74	80	0	303
s71	32	25	632	0
s72	86	4	277	0
s73	66	86	0	68

Table A6. Site 6 heat streams.

Stream	T^{in} [°C]	T^{out} [°C]	H^{in} [kW]	H^{out} [kW]
s1	5	35	0	36.88
s2	15	35	0	1064.17
s3	36	35	0	−305.55
s4	36	100	0	273.15
s5	100	100	0	2297.7
s6	36	90	0	115.9
s7	148	25	0	−883.18
s8	115	115	0	−391.55
s9	148	148	0	−3622.26
s10	115	25	0	−66.94
s11	100	25	0	−106.43
s12	100	100	0	−767.76
s13	50	138	0	270.27
s14	138	144	0	9.35
s15	138	138	0	1560.4
s16	77	78	0	391.25
s17	5	89	0	599.1
s18	5	78	0	67.25
s19	78	115	0	574.64
s20	5	48	0	1571.1
s21	5	78	0	134.49
s22	51	48	0	−397.36
s23	51	89	0	140.6
s24	5	48	0	85.59
s25	40	40	0	76.23
s26	5	138	0	38.88
s27	35	40	0	114.35

Table A6. *Cont.*

Stream	T^{in} [°C]	T^{out} [°C]	H^{in} [kW]	H^{out} [kW]
s28	5	40	0	11.43
s29	138	138	0	151.7
s30	70	99	0	0.59
s31	52	20	0	−0.42
s32	51	20	0	−0.07
s33	20	51	0	0.07
s34	20	99	0	0.77
s35	99	130	0	2.45
s36	51	59	0	0.15
s37	49	20	0	−0.55
s38	51	59	0	0.15
s39	49	20	0	−0.55
s40	20	100	0	0.13
s41	20	49	0	0.55
s42	20	50	0	0.04
s43	20	50	0	0.04
s44	20	59	0	0.01
s45	20	59	0	0.01
s46	51	20	0	−0.07
s47	50	20	0	−0.04
s48	50	20	0	−0.04
s49	20	49	0	0.55
s50	20	51	0	0.07
s51	85	85	2.27	0
s52	88	88	0.57	0
s53	88	20	0.05	0
s54	84	20	0.05	0
s55	54	54	0	1.77
s56	54	54	0	0.46
s57	108	108	0	0.49
s58	103	103	0	2.3
s59	99	20	0.34	0
s60	71	20	0.05	0
s61	69	20	0.04	0
s62	79	20	0.08	0
s63	54	20	0.11	0
s64	54	20	0.03	0
s65	85	85	0	2.34
s66	88	88	0	0.54
s67	70	70	1.76	0
s68	70	20	0.16	0
s69	71	71	0	0.75
s70	70	70	0	2.03
s71	62	62	0.66	0
s72	84	84	0	0.45
s73	88	88	0.39	0
s74	62	62	0	0.54

Table A6. *Cont.*

Stream	T^{in} [°C]	T^{out} [°C]	H^{in} [kW]	H^{out} [kW]
s75	69	69	0.47	0
s76	71	71	0.59	0
s77	99	99	2.3	0
s78	88	20	0.07	0
s79	84	84	0.44	0
s80	69	69	0	0.5
s81	54	54	1.81	0
s82	88	88	0	0.54
s83	79	79	0	0.91
s84	62	20	0.05	0
s85	108	108	0.48	0
s86	79	79	0.79	0
s87	108	20	0.08	0
s88	54	54	0.43	0
s89	85	20	0.27	0
s90	100	100	1.72	0
s91	58	90	0	0.11
s92	100	100	0	1.61
s93	20	61	0	0.02
s94	20	69	0	0.02
s95	47	61	0	0.31
s96	53	69	0	0.26
s97	20	160	0	0.29

Table A7. Site 7 heat streams.

Stream	T^{in} [°C]	T^{out} [°C]	H^{in} [kW]	H^{out} [kW]
s1	25	110	0	72.53
s2	145	145	0	359.51
s3	180	180	0	28.07
s4	160	180	0	141.91
s5	110	150	0	97.76
s6	70	70	0	116.68
s7	180	190	0	141.91
s8	66	64	3.15	0
s9	141	141	0	−6.31
s10	58	55	3.15	0
s11	86	75	15.77	0
s12	132	123	15.77	0
s13	65	65	0	34.69
s14	189	160	12.61	0
s15	25	26	0	9.46
s16	139	133	12.61	0
s17	108	99	15.77	0
s18	62	59	3.15	0
s19	99	95	15.77	0
s20	93	77	12.61	0

Table A7. *Cont.*

Stream	T^{in} [°C]	T^{out} [°C]	H^{in} [kW]	H^{out} [kW]
s21	139	138	6.31	0
s22	178	175	9.46	0
s23	153	132	15.77	0
s24	118	114	15.77	0
s25	59	58	3.15	0
s26	181	178	9.46	0
s27	146	139	12.61	0
s28	63	63	0	25.23
s29	69	66	3.15	0
s30	112	106	12.61	0
s31	152	130	15.77	0
s32	145	143	6.31	0
s33	120	114	15.77	0
s34	180	180	0	44.15
s35	140	139	6.31	0
s36	140	140	0	−6.31
s37	125	112	12.61	0
s38	175	167	9.46	0
s39	78	54	12.61	0
s40	55	52	3.15	0
s41	148	138	12.61	0
s42	75	53	15.77	0
s43	128	124	12.61	0
s44	113	104	15.77	0
s45	110	110	0	15.77
s46	95	86	15.77	0
s47	160	146	12.61	0
s48	25	26	0	18.92
s49	178	152	15.77	0
s50	52	45	3.15	0
s51	77	46	12.61	0
s52	134	128	12.61	0
s53	84	61	15.77	0
s54	114	108	15.77	0
s55	123	118	15.77	0
s56	119	114	12.61	0
s57	63	110	0	25.23
s58	114	104	12.61	0
s59	142	141	6.31	0
s60	143	142	6.31	0
s61	138	134	12.61	0
s62	130	120	15.77	0
s63	104	100	15.77	0
s64	100	93	15.77	0
s65	93	84	15.77	0
s66	110	112	0	47.3
s67	64	63	3.15	0

Table A7. *Cont.*

Stream	T^{in} [°C]	T^{out} [°C]	H^{in} [kW]	H^{out} [kW]
s68	114	113	15.77	0
s69	133	125	12.61	0
s70	104	94	12.61	0
s71	106	93	12.61	0
s72	141	140	6.31	0
s73	141	141	0	−6.31
s74	75	69	3.15	0
s75	124	119	12.61	0
s76	94	78	12.61	0
s77	63	62	3.15	0
s78	141	141	0	−6.31
s79	25	26	0	132.45
s80	25	26	0	91.45
s81	550	500	100.91	0
s82	350	340	31.54	0
s83	75	75	0	56.76
s84	80	80	0	22.08
s85	80	115	0	22.08
s86	150	160	0	72.53
s87	170	180	0	72.53
s88	190	200	0	37.84
s89	160	170	0	72.53
s90	120	29	126.14	0
s91	305	300	9.46	0
s92	320	310	50.46	0
s93	25	26	0	15.77
s94	79	50	97.76	0
s95	75	80	0	12.61
s96	120	120	0	41
s97	25	26	0	22.08
s98	340	330	15.77	0
s99	550	550	0	−100.91
s100	157	120	167.14	0
s101	214	140	135.6	0
s102	50	41	63.07	0
s103	168	120	69.38	0
s104	180	190	0	110.38
s105	140	94	75.69	0
s106	120	33	25.23	0
s107	330	320	25.23	0
s108	310	305	31.54	0
s109	150	155	0	25.23
s110	160	185	0	18.92
s111	120	125	0	25.23
s112	166	170	0	37.84
s113	185	190	0	28.38
s114	135	145	0	28.38

Table A7. *Cont.*

Stream	T^{in} [°C]	T^{out} [°C]	H^{in} [kW]	H^{out} [kW]
s115	110	110	0	56.76
s116	97	100	0	9.46
s117	93	95	0	53.61
s118	185	185	0	47.3
s119	125	130	0	47.3
s120	155	166	0	12.61
s121	130	135	0	37.84
s122	25	26	0	22.08
s123	90	92	0	18.92
s124	145	150	0	31.54
s125	110	45	47.3	0
s126	95	97	0	63.07
s127	92	93	0	34.69
s128	65	35	227.06	0
s129	25	26	0	15.77
s130	114	45	72.53	0
s131	180	190	0	28.38
s132	160	180	0	28.38
s133	60	60	0	217.6
s134	130	130	0	25.23
s135	25	26	0	22.08
s136	118	129	0	31.54
s137	185	190	0	34.69
s138	129	134	0	12.61
s139	25	26	0	15.77
s140	93	29	47.3	0
s141	73	44	230.21	0
s142	160	185	0	34.69
s143	295	295	0	−3.15
s144	116	118	0	18.92
s145	104	48	85.15	0
s146	185	185	0	72.53
s147	218	217	56.76	0
s148	325	315	6.31	0
s149	99	35	28.38	0
s150	315	315	0	−31.54
s151	180	180	0	56.76
s152	165	170	0	28.38
s153	295	290	56.76	0
s154	204	203	91.45	0
s155	25	26	0	6.31
s156	80	85	0	12.61
s157	79	45	258.59	0
s158	615	615	0	−280.67
s159	50	29	25.23	0
s160	135	145	0	56.76
s161	312	300	37.84	0

Table A7. *Cont.*

Stream	T^{in} [°C]	T^{out} [°C]	H^{in} [kW]	H^{out} [kW]
s162	203	197	22.08	0
s163	49	49	0	34.69
s164	125	125	0	189.21
s165	171	130	37.84	0
s166	138	60	88.3	0
s167	130	135	0	28.38
s168	130	45	69.38	0
s169	150	160	0	28.38
s170	125	130	0	28.38
s171	170	180	0	28.38
s172	25	26	0	9.46
s173	145	150	0	44.15
s174	300	295	56.76	0
s175	180	180	0	−31.54
s176	160	165	0	44.15
s177	315	314	18.92	0
s178	60	70	0	12.61
s179	70	80	0	15.77
s180	127	127	0	15.77
s181	75	76	0	18.92
s182	314	312	18.92	0
s183	59	45	56.76	0
s184	160	160	0	15.77
s185	115	125	0	22.08
s186	170	180	0	47.3
s187	115	115	0	88.3
s188	180	190	0	18.92
s189	78	45	113.53	0
s190	25	26	0	9.46
s191	170	170	0	28.38
s192	85	85	0	15.77
s193	25	26	0	15.77
s194	70	45	59.92	0
s195	94	34	85.15	0
s196	120	29	81.99	0
s197	180	60	5695.03	0
s198	60	25	1601.73	0
s199	900	340	25627.65	0

Appendix A.2 Cement Fuel Properties

Table A8 depicts the LHV, share in the fuel mix and price of the fuels used in cement production.

Table A8. Cement fuel properties, shares and parices.

Fuel	LHV [kJ/kg]	Share [%]	Price [€/kg]
Coal	28066	10.5	60
Lignite	9500	23.8	11

Table A8. *Cont.*

Fuel	LHV [kJ/kg]	Share [%]	Price [€/kg]
Petcoke	32701	3.4	83
Fuel oil	40800	0.3	413
Tyres	30000	9.2	10
Waste oil	35000	2.5	10
Waste paper	17000	1.1	20
Waste plastic	20000	10.1	20
Waste textile	35000	0.4	20
Other waste	6000	18.7	20
Animal meal	20000	4	5
Sewage	15000	12.3	10
Scrap wood	17000	0.1	20
Solvents	25000	2.8	20

References

1. European Comission. *Europe 2020*; Technical Report; European Comission: Brussels, Belgium, 2010.
2. EIA—U.S. Energy Information Administration. *International Energy Outlook 2017*; Technical Report; EIA: Washington, DC, USA, 2017.
3. *Final Energy Consumption by Sector and Fuel*; European Energy Agency (EEA): Copenhagen, Denmark, 2018.
4. Bendig, M.; Maréchal, F.; Favrat, D. Defining "Waste Heat" for industrial processes. *Appl. Therm. Eng.* **2013**, *61*, 134–142. [CrossRef]
5. Miró, L.; Brückner, S.; Cabeza, L.F. Mapping and discussing Industrial Waste Heat (IWH) potentials for different countries. *Renew. Sustain. Energy Rev.* **2015**, *51*, 847–855. [CrossRef]
6. Bertnsson, T.; Asblad, A. *Industrial Excess Heat Recovery—Technologies and Applications*; Technical Report; IEA—International Energy Agency: Copenhagen, Denmark, 2015.
7. Suciu, R.; Girardin, L.; Maréchal, F. Energy integration of CO_2 networks and power to gas for emerging energy autonomous cities in Europe. *Energy* **2018**, *157*, 830–842. [CrossRef]
8. Oliveira, C.M.; Pavão, L.V.; Ravagnani, M.A.; Cruz, A.J.; Costa, C.B. Process integration of a multiperiod sugarcane biorefinery. *Appl. Energy* **2018**, *213*, 520–539. [CrossRef]
9. Linnhoff, B.; Hindmarsh, E. The pinch design method for heat exchanger networks. *Chem. Eng. Sci.* **1983**, *38*, 745–763. [CrossRef]
10. Dhole, V.R.; Linnhoff, B. Total site targets for fuel, co-generation, emissions, and cooling. *Comput. Chem. Eng.* **1993**, *17*, S101–S109. [CrossRef]
11. Hu, C.; Ahmad, S. Total site heat integration using the utility system. *Comput. Chem. Eng.* **1994**, *18*, 729–742. [CrossRef]
12. Pirmohamadi, A.; Ghazi, M.; Nikian, M. Optimal design of cogeneration systems in total site using exergy approach. *Energy* **2019**, *166*, 1291–1302. [CrossRef]
13. Liew, P.Y.; Wan Alwi, S.R.; Ho, W.S.; Abdul Manan, Z.; Varbanov, P.S.; Klemeš, J.J. Multi-period energy targeting for Total Site and Locally Integrated Energy Sectors with cascade Pinch Analysis. *Energy* **2018**, *155*, 370–380. [CrossRef]
14. Song, R.; Wang, Y.; Panu, M.; El-Halwagi, M.M.; Feng, X. Improved Targeting Procedure To Determine the Indirect Interplant Heat Integration with Parallel Connection Pattern among Three Plants. *Ind. Eng. Chem. Res.* **2018**, *57*, 1569–1580. [CrossRef]
15. Wang, Y.; Feng, X.; Chu, K.H. Trade-off between energy and distance related costs for different connection patterns in heat integration across plants. *Appl. Therm. Eng.* **2014**, *70*, 857–866. [CrossRef]
16. Song, R.; Feng, X.; Wang, Y. Feasible heat recovery of interplant heat integration between two plants via an intermediate medium analyzed by Interplant Shifted Composite Curves. *Appl. Therm. Eng.* **2016**, *94*, 90–98. [CrossRef]

17. Hackl, R.; Andersson, E.; Harvey, S. Targeting for energy efficiency and improved energy collaboration between different companies using total site analysis (TSA). *Energy* **2011**, *36*, 4609–4615. [CrossRef]
18. Hackl, R.; Harvey, S. From heat integration targets toward implementation—A TSA (total site analysis)-based design approach for heat recovery systems in industrial clusters. *Energy* **2015**, *90*, 163–172. [CrossRef]
19. Morandin, M.; Hackl, R.; Harvey, S. Economic feasibility of district heating delivery from industrial excess heat: A case study of a Swedish petrochemical cluster. *Energy* **2014**, *65*, 209–220. [CrossRef]
20. Chew, K.H.; Klemeš, J.J.; Wan Alwi, S.R.; Abdul Manan, Z. Industrial implementation issues of Total Site Heat Integration. *Appl. Therm. Eng.* **2013**, *61*, 17–25. [CrossRef]
21. Liew, P.Y.; Wan Alwi, S.R.; Klemeš, J.J. Total Site Heat Integration Targeting Algorithm Incorporating Plant Layout Issues. In *Computer Aided Chemical Engineering*; Elsevier: Amsterdam, The Netherlands, 2014; Volume 33, pp. 1801–1806, doi:10.1016/B978-0-444-63455-9.50135-5.
22. Papoulias, S.A.; Grossmann, I.E. A structural optimization approach in process synthesis—II. *Comput. Chem. Eng.* **1983**, *7*, 707–721. [CrossRef]
23. Cerda, J.; Westerburg, A.W. Synthesizing Heat Exchanger Networks Having Restricted Stream/Stream Matches Using a Transportation Problem Formulation. *Chem. Eng. Sci.* **1983**, *38*, 1723–1740. [CrossRef]
24. Yee, T.; Grossmann, I. Simultaneous optimization models for heat integration—II. Heat exchanger network synthesis. *Comput. Chem. Eng.* **1990**, *14*, 1165–1184. [CrossRef]
25. Zhang, B.; Li, J.; Zhang, Z.; Wang, K.; Chen, Q. Simultaneous design of heat exchanger network for heat integration using hot direct discharges/feeds between process plants. *Energy* **2016**, *109*, 400–411. [CrossRef]
26. Wang, Y.; Chang, C.; Feng, X. A systematic framework for multi-plants Heat Integration combining Direct and Indirect Heat Integration methods. *Energy* **2015**, *90*, 56–67. [CrossRef]
27. Rodera, H.; Bagajewicz, M.J. Targeting procedures for energy savings by heat integration across plants. *AIChE J.* **1999**, *45*, 1721–1742. [CrossRef]
28. Bagajewicz, M.; Rodera, H. Energy savings in the total site heat integration across many plants. *Comput. Chem. Eng.* **2000**, *24*, 1237–1242. [CrossRef]
29. Bagajewicz, M.J.; Barbaro, A.F. On the use of heat pumps in total site heat integration. *Comput. Chem. Eng.* **2003**, *27*, 1707–1719. [CrossRef]
30. Stijepovic, M.Z.; Linke, P. Optimal waste heat recovery and reuse in industrial zones. *Energy* **2011**, *36*, 4019-4031. [CrossRef]
31. Kantor, I.; Betancourt, A.; Elkamel, A.; Fowler, M.; Almansoori, A. Generalized mixed-integer nonlinear programming modeling of eco-industrial networks to reduce cost and emissions. *J. Clean. Prod.* **2015**, *99*, 160–176. [CrossRef]
32. Becker, H.; Maréchal, F. Energy integration of industrial sites with heat exchange restrictions. *Comput. Chem. Eng.* **2012**, *37*, 104–118. [CrossRef]
33. Pouransari, N.; Maréchal, F. Heat recovery networks synthesis of large-scale industrial sites: Heat load distribution problem with virtual process subsystems. *Energy Convers. Manag.* **2015**, *89*, 985–1000. [CrossRef]
34. Bade, M.H.; Bandyopadhyay, S. Minimization of Thermal Oil Flow Rate for Indirect Integration of Multiple Plants. *Ind. Eng. Chem. Res.* **2014**, *53*, 13146–13156. [CrossRef]
35. Furman, K.C.; Sahinidis, N.V. A Critical Review and Annotated Bibliography for Heat Exchanger Network Synthesis in the 20th Century. *Ind. Eng. Chem. Res.* **2002**, *41*, 2335–2370. [CrossRef]
36. Song, R.; Tang, Q.; Wang, Y.; Feng, X.; El-Halwagi, M.M. The implementation of inter-plant heat integration among multiple plants. Part I: A novel screening algorithm. *Energy* **2017**, *140*, 1018–1029. [CrossRef]
37. Song, R.; Chang, C.; Tang, Q.; Wang, Y.; Feng, X.; El-Halwagi, M.M. The implementation of inter-plant heat integration among multiple plants. Part II: The mathematical model. *Energy* **2017**, *135*, 382–393. [CrossRef]
38. Chang, C.; Chen, X.; Wang, Y.; Feng, X. An efficient optimization algorithm for waste Heat Integration using a heat recovery loop between two plants. *Appl. Therm. Eng.* **2016**, *105*, 799–806. [CrossRef]
39. Chang, C.; Chen, X.; Wang, Y.; Feng, X. Simultaneous optimization of multi-plant heat integration using intermediate fluid circles. *Energy* **2017**, *121*, 306–317. [CrossRef]
40. Nair, S.K.; Soon, M.; Karimi, I. Locating exchangers in an EIP-wide heat integration network. *Comput. Chem. Eng.* **2018**, *108*, 57–73. [CrossRef]
41. Kachacha, C.; Farhat, A.; Zoughaib, A.; Tran, C.T. Site wide heat integration in eco-industrial parks considering variable operating conditions. *Comput. Chem. Eng.* **2019**, *126*, 304–320. [CrossRef]

42. Laukkanen, T.; Seppälä, A. Interplant heat exchanger network synthesis using nanofluids for interplant heat exchange. *Appl. Therm. Eng.* **2018**, *135*, 133–144. [CrossRef]
43. Liu, L.; Song, H.; Zhang, L.; Du, J. Heat-integrated water allocation network synthesis for industrial parks with sequential and simultaneous design. *Comput. Chem. Eng.* **2018**, *108*, 408–424. [CrossRef]
44. Marechal, F.; Kalitventzeff, B. Targeting the integration of multi-period utility systems for site scale process integration. *Appl. Therm. Eng.* **2003**, *23*, 1763–1784. [CrossRef]
45. Chang, C.; Wang, Y.; Ma, J.; Chen, X.; Feng, X. An energy hub approach for direct interplant heat integration. *Energy* **2018**, *159*, 878–890. [CrossRef]
46. Bohm, B. On transient heat losses from buried district heating pipes. *Int. J. Energy Res.* **2000**, *24*, 1311–1334. [CrossRef]
47. Haaland, S.E. Simple and Explicit Formulas for the Friction Factor in Turbulent Pipe Flow. *J. Fluids Eng.* **1983**, *105*, 89. [CrossRef]
48. Genic, S.; Arandelovic, I.; Kolendic, P.; Jaric, M.; Budimir, N.; Genic, V. A review of explicit approximations of Colebrook's equation. *FME Trans.* **2011**, *39*, 67–71.
49. Nowak, I. *Relaxation and Decomposition Methods for Mixed Integer Nonlinear Programming*; Number v. 152 in International Series of Numerical Mathematics; OCLC: ocm61228819; Birkhäuser: Boston, MA, USA, 2005.
50. Yildirim, N.; Toksoy, M.; Gokcen, G. Piping network design of geothermal district heating systems: Case study for a university campus. *Energy* **2010**, *35*, 3256–3262. [CrossRef]
51. Kwak, D.H.; Binns, M.; Kim, J.K. Integrated design and optimization of technologies for utilizing low grade heat in process industries. *Appl. Energy* **2014**, *131*, 307–322. [CrossRef]
52. Alva-Argáez, A.; Kokossis, A.C.; Smith, R. The design of water-using systems in petroleum refining using a water-pinch decomposition. *Chem. Eng. J.* **2007**, *128*, 33–46. [CrossRef]
53. Nordman, R.; Berntsson, T. Use of advanced composite curves for assessing cost-effective HEN retrofit II. Case studies. *Appl. Therm. Eng.* **2009**, *29*, 282–289. [CrossRef]
54. Persson, J.; Berntsson, T. Influence of short-term variations on energy-saving opportunities in a pulp mill. *J. Clean. Prod.* **2010**, *18*, 935–943. [CrossRef]
55. Nussbaumer, T.; Thalmann, S. Influence of system design on heat distribution costs in district heating. *Energy* **2016**, *101*, 496–505. [CrossRef]
56. Bütün, H.; Kantor, I.; Maréchal, F. A heat integration method with multiple heat exchange interfaces. *Energy* **2018**, *152*, 476–488. [CrossRef]
57. Galitsky, C.; Martin, N.; Worrell, E.; Lehman, B. *Energy Efficiency Improvement and Cost Saving Opportunities for Breweries: An ENERGY STAR® Guide for Energy and Plant Managers*; Technical Report; Lawrence Berkeley National Lab. (LBNL): Berkeley, CA, USA, 2003.
58. Marechal, F.; Sachan, A.K.; Salgueiro, L. Application of Process Integration Methodologies in the Brewing Industry. In *Handbook of Process Integration (PI)*; Elsevier: Cambridge, UK, 2013; pp. 820–863. [CrossRef]
59. Kantor, I.; Wallerand, A.S.; Kermani, M.; Bütün, H.; Santecchia, A.; Norbert, R.; Cervo, H.; Arias, S.; Wolf, F.; Van Eetvelde, G.; et al. Thermal profile construction for energy-intensive industrial sectors. In Proceedings of the ECOS 2018—The 31st International Conference on Efficiency, Cost, Optimization, Simulation and Environmental Impact of Energy Systems, Guimaraes, Portugal, 17–22 June 2018.
60. Brown, D.; Maréchal, F.; Paris, J. A dual representation for targeting process retrofit, application to a pulp and paper process. *Appl. Therm. Eng.* **2005**, *25*, 1067–1082. [CrossRef]
61. Maréchal, F.; Kalitventzeff, B. Process integration: Selection of the optimal utility system. *Comput. Chem. Eng.* **1998**, *22*, S149–S156. [CrossRef]
62. Maréchal, F.; Kalitventzeff, B. Targeting the optimal integration of steam networks: Mathematical tools and methodology. *Comput. Chem. Eng.* **1999**, *23*, S133–S136. [CrossRef]
63. Ponce-Ortega, J.M.; Serna-González, M.; Jiménez-Gutiérrez, A. Optimization model for re-circulating cooling water systems. *Comput. Chem. Eng.* **2010**, *34*, 177–195. [CrossRef]
64. Turton, R.; Bailie, R.C.; Whiting, W.B.; Shaeiwitz, J.A.; Bhattacharya, D. *Analysis, Synthesis, and Design of Chemical Processes*, 4th ed.; Prentice Hall: Upper Saddle River, NJ, USA, 2012.
65. Bernard, D.; Lemarchand, D.; Tétreault, N.; Theévenet, C. *Increasing the Use of Alternative Fuels at Cement Plants: International Best Practice*; Technical Report; International Finance Corporation: Washington, DC, USA, 2017.

66. Verein Deutscher Zementwerke. *Environmental Data of the Germand Cement Industry*; Technical Report; Environmental Data of the German Cement Industry: Düsseldorf, Germany, 2013.
67. Office of Energy Efficiency Industrial, Commercial and Institutional Programs. *Energy Consumption Benchmark Guide: Cement Clinker Production*; Technical Report; Natural Resources Canada: Ottawa, ON, Canada, 2001.